CHAPTER IV
RESULTS AND DISCUSSION

The adsorption isotherms and contact angle measurements for the solutions of CPB, $OP(EO)_{10}$, and their mixtures with the various molar fraction of $OP(EO)_{10}$ in the mixed surfactant solution (α); 0.25, 0.50, and 0.75 were done on six plastic surfaces; HDPE, PC, PVC, ABS, PMMA, and Nylon66. Furthermore, the surface tension (γ_{LV}) for the solutions of CPB, $OP(EO)_{10}$, and their mixtures was also measured.

4.1 Contact Angle of Water and Specific Surface Area of Plastics

The contact angle of water on plastics and the specific surface area of plastics used in this work are shown in Table 4.1.

Table 4.1 Contact angle of water and the specific surface area of HDPE, PVC, PC, ABS, PMMA, and Nylon66

Plastics	Contact angle of water (degree)	Specific Surface Area (m^2/g)
HDPE	92.78	1.443
PC	89.63	1.640
PVC	84.24	1.812
ABS	83.86	3.103
PMMA	77.56	1.012
Nylon66	69.80	6.353

As shown in Table 4.1, all studied plastic samples have extremely low specific surface areas. The contact angle of pure water on HDPE is the highest and follows by PC, PVC, ABS, PMMA, and Nylon66, respectively. This result indicates that the degree of hydrophobicity of plastics increases in the order of:

HDPE > PC > PVC > ABS > PMMA > Nylon66.

4.2 The Interfacial Tension at Liquid/Vapor Interface and CMC for the Solutions of CPB, $OP(EO)_{10}$, and Their Mixtures

The surface tension isotherms of CPB, $OP(EO)_{10}$, and their mixtures are shown in Fig. 4.1. For any given surfactant system, the γ_{LV} decreased with increasing surfactant concentration and remained almost unchanged after reaching the CMC. The CMC values determined from the inflections in the isotherms are listed in Table 4.2. The CMC of the cationic surfactant (CPB) solution decreases with increasing molar fraction of the nonionic surfactant.

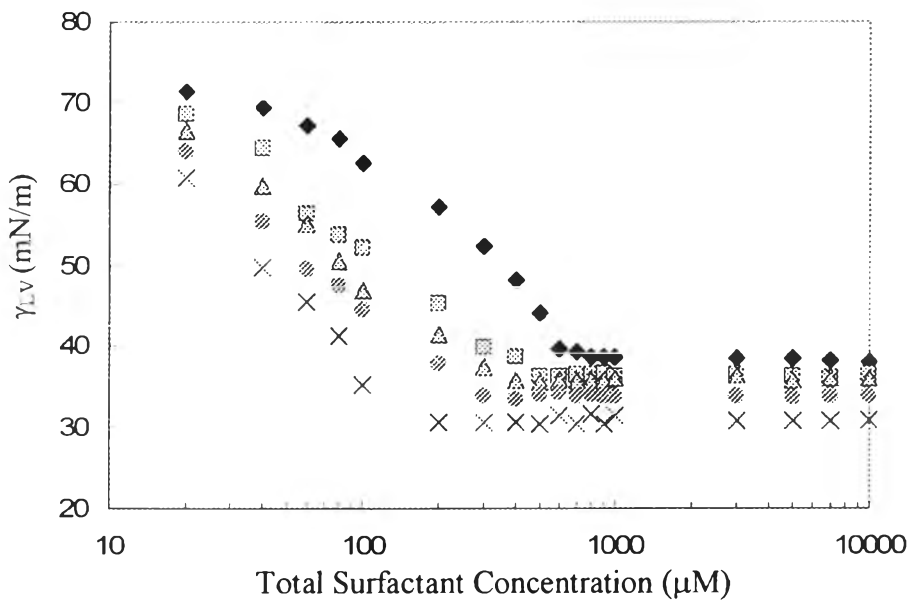

Figure 4.1 Surface tension isotherms for the solutions of (♦) CPB, (×) $OP(EO)_{10}$, and their mixtures with α = (■) 0.25, (▲) 0.50, and (●) 0.75.

Table 4.2 CMC values for mixed CPB– $OP(EO)_{10}$ solutions at different $OP(EO)_{10}$ molar fractions (α)

α	CMC (M)
0	6.0×10^{-4}
0.25	5.0×10^{-4}
0.50	4.0×10^{-4}
0.75	3.0×10^{-4}
1.0	2.0×10^{-4}

4.2 Adsorption and Wettability on Plastic Surfaces by Solution of CPB, $OP(EO)_{10}$, and their Mixtures

4.3.1 Mixed Surfactant Adsorption Isotherms

The adsorption isotherms for the solutions of CPB, $OP(EO)_{10}$, and their mixtures with α was 0.25, 0.50, and 0.75 on HDPE, PC, PVC, ABS, PMMA, and Nylon66 are shown in Figure 4.2 – 4.7. Surfactant adsorption on plastic surfaces was calculated from the difference between the initial (C_o, μM) and equilibrium (C, μM) solution concentrations by the following formula:

$$\Gamma = \frac{(C_0 - C)V}{W_{plastic} a_s}, \qquad (4.1)$$

where V is the volume of a surfactant solution, l; $W_{plastic}$ is the weight of a powdered plastic sample, g; and a_s is the specific surface area of the powdered plastic sample, m^2/g (Kharitonova *et al.*, 2005).

For all plastic surfaces, the surfactant adsorption increased with increasing surfactant concentration and reached the plateau at about the CMC which the maximum surfactant adsorption could be determined. For any given plastic, the

maximum surfactant adsorption of the pure CPB solution was less than that of the pure $OP(EO)_{10}$ solution. For mixed surfactant solutions, their maximum adsorptions were in between the pure surfactant systems. For any non-polar plastic surface and any given nonionic surfactant ratio, the maximum surfactant adsorption was lower than that of any slightly polar plastic surface. Moreover, the presence of nonionic surfactant in the mixtures showed the positive effect in adsorption because of the reduction of electrostatic repulsion between the head groups of adsorbed cationic surfactant molecules (Rosen, 2004, and Somasundaran *et al.*, 1996).

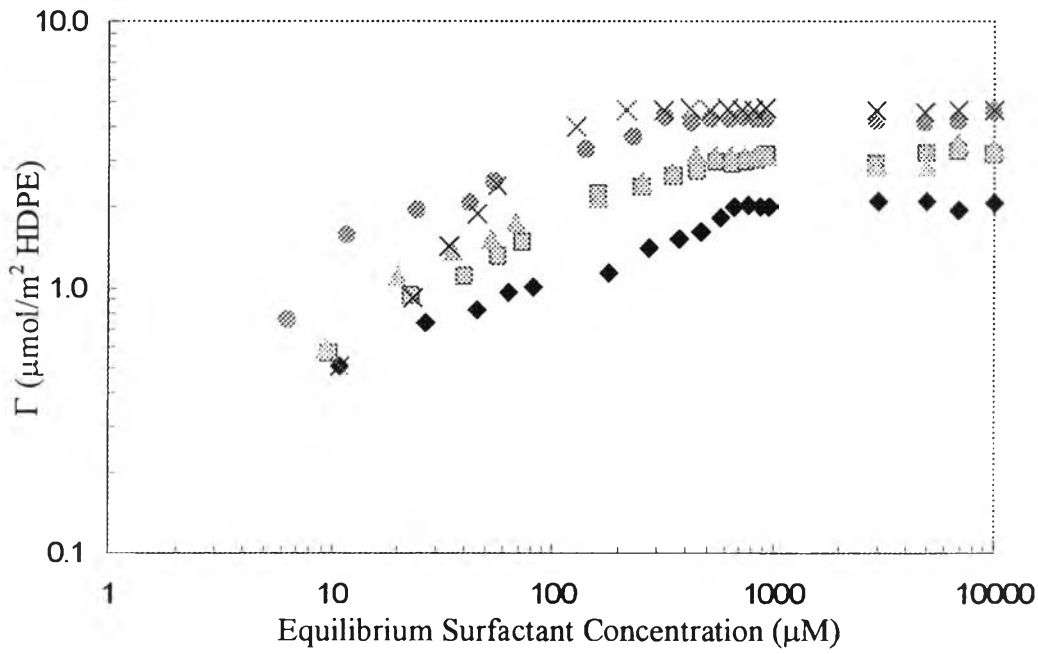

Figure 4.2 Adsorption isotherm for solutions of (♦) CPB, (×) $OP(EO)_{10}$, and their mixtures with α = (■) 0.25, (▲) 0.50, and (●) 0.75 on HDPE.

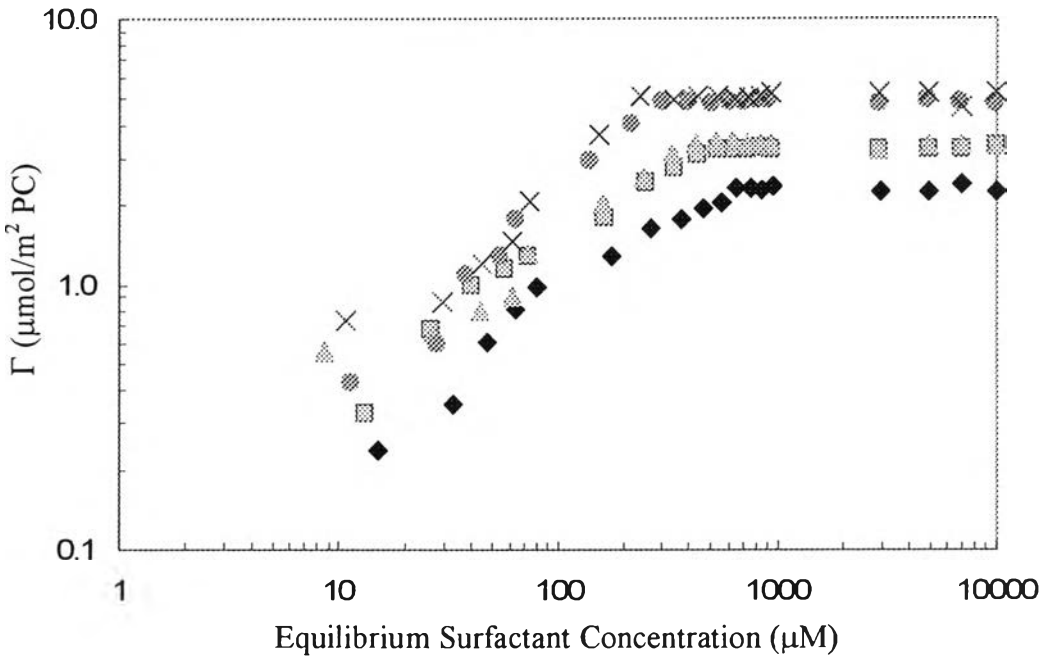

Figure 4.3 Adsorption isotherm for solutions of (♦) CPB, (×) $OP(EO)_{10}$, and their mixtures with α = (■) 0.25, (▲) 0.50, and (●) 0.75 on PC.

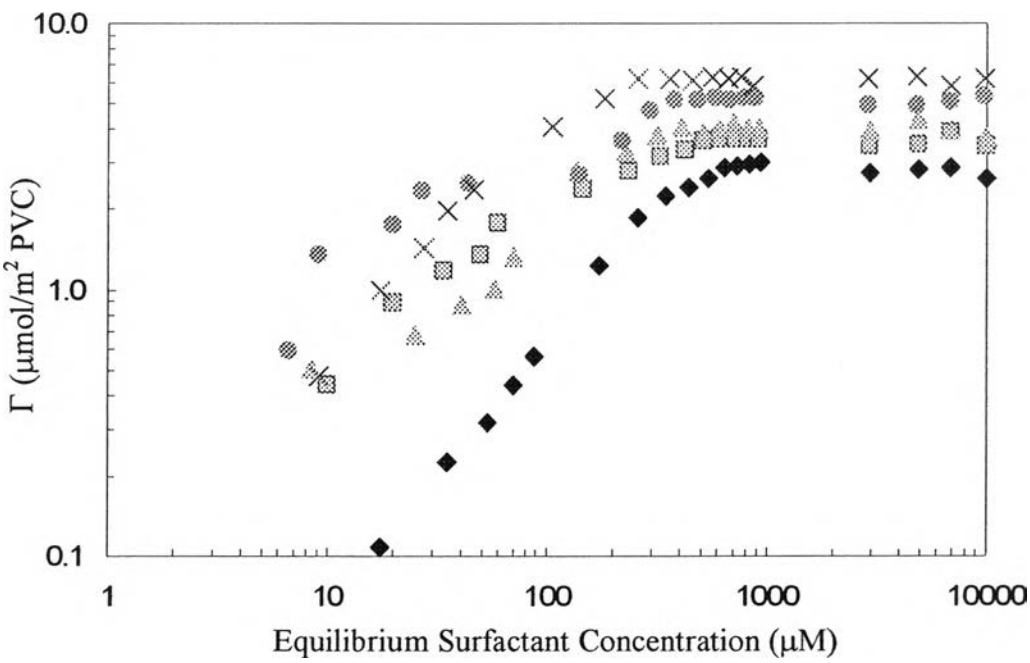

Figure 4.4 Adsorption isotherm for solutions of (♦) CPB, (×) $OP(EO)_{10}$, and their mixtures with α = (■) 0.25, (▲) 0.50, and (●) 0.75 on PVC.

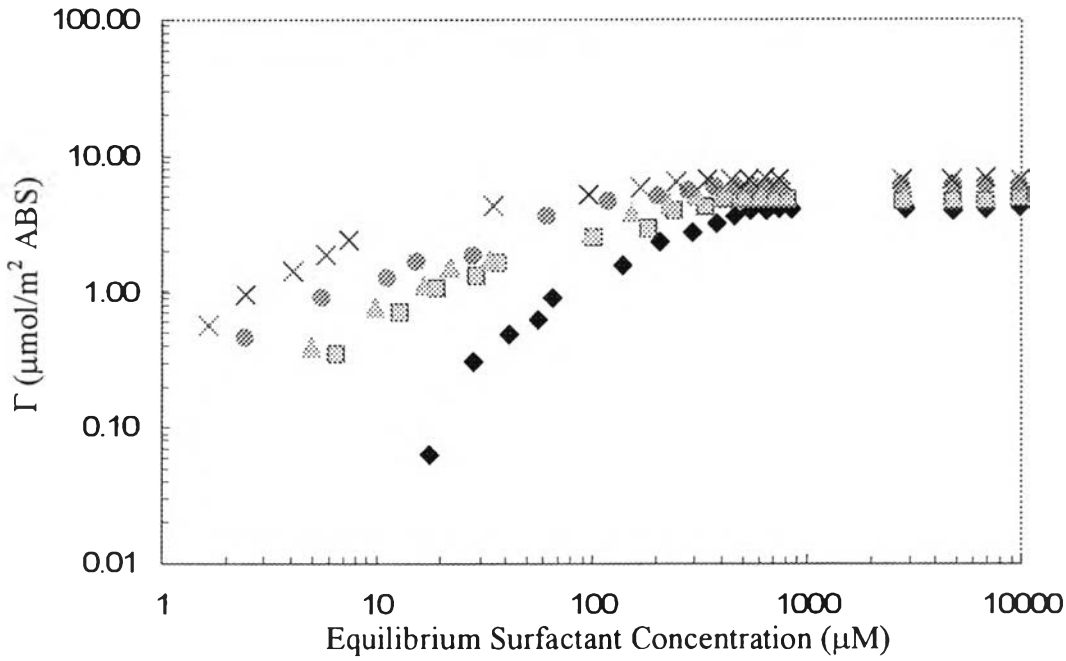

Figure 4.5 Adsorption isotherm for solutions of (♦) CPB, (×) $OP(EO)_{10}$, and their mixtures with α = (■) 0.25, (▲) 0.50, and (●) 0.75 on ABS.

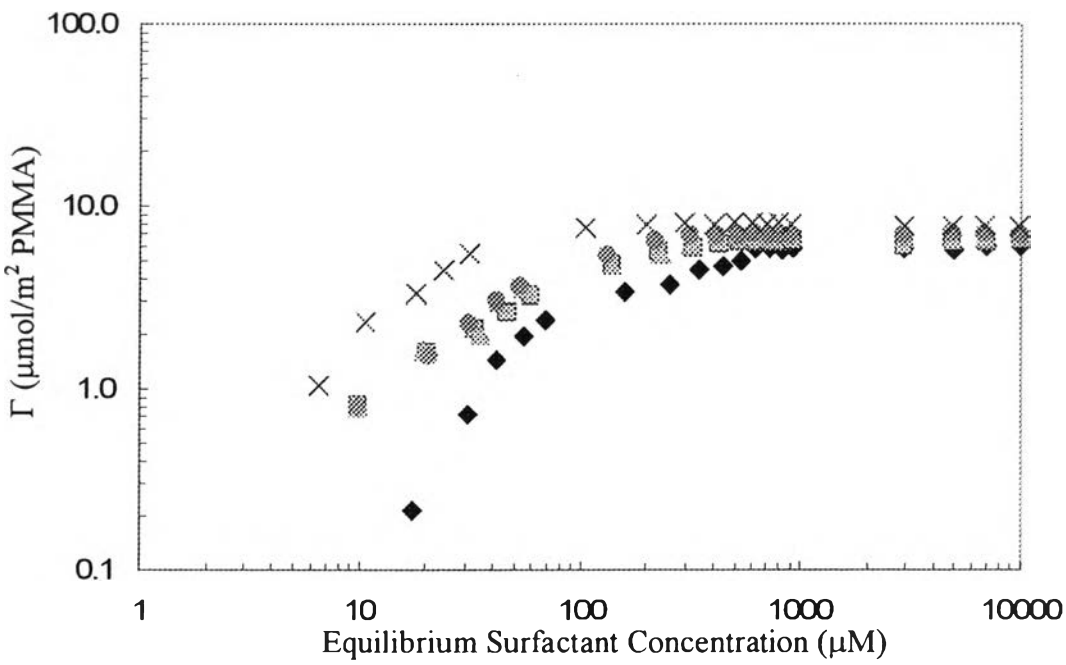

Figure 4.6 Adsorption isotherm for solutions of (♦) CPB, (×) $OP(EO)_{10}$, and their mixtures with α = (■) 0.25, (▲) 0.50, and (●) 0.75 on PMMA.

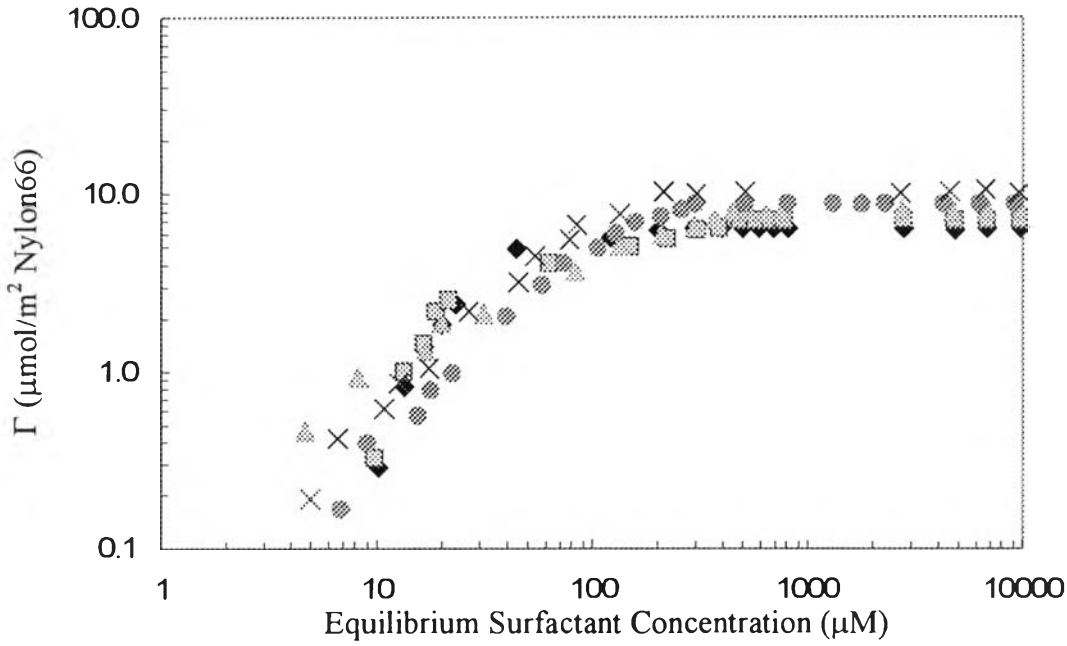

Figure 4.7 Adsorption isotherm for solutions of (♦) CPB, (×) $OP(EO)_{10}$, and their mixtures with α = (■) 0.25, (▲) 0.50, and (●) 0.75 on Nylon66.

For the mixed surfactant systems, the concentrations of cationic surfactant, CPB, and that of nonionic surfactant, $OP(EO)_{10}$ were determined by using a UV-Vis spectrophotometer (Shimadzu, UV-2550) at wavelengths of 254, and 282 nm, respectively, in which the pyridinium and the phenyl groups have strong adsorption bands. CPB and $OP(EO)_{10}$ adsorption isotherms from the single solutions and the mixtures on HDPE, PC, PVC, ABS, PMMA and Nylon66 are presented in Figure 4.8-4.19. It is seen from these figures that CPB adsorption was enhanced by the presence of nonionic surfactant as indicated by the shift of CPB isotherms toward the left with increasing in molar fractions of nonionic surfactants.

For any given plastic surface, the maximum CPB adsorption from the experiment was higher than that from the calculation when $OP(EO)_{10}$ was added into the CPB solutions (see Table 4.3). The result suggests that the presence of nonionic surfactant in the CPB solution provided positive effect in adsorption because of the reduction of electrostatic repulsion between the head groups of adsorbed cationic surfactant molecules (Rosen, 2004, and Somasundaran *et al.*, 1996).

Contrary, the maximum amounts of $OP(EO)_{10}$ adsorbed obtained at the plateau region from the mixtures on different plastic surfaces are shown in Table 4.4. The maximum $OP(EO)_{10}$ adsorption from the experiment was less than that of the calculation when CPB presented in the $OP(EO)_{10}$ solutions. The possible reason is the masking of negative charge plastic surfaces by the CPB monomeric adsorption obstructed the $OP(EO)_{10}$ adsorption (Desai and Dixit, 1996).

Table 4.3 Maximum CPB adsorption, ($\mu mol/m^2$ of plastic), of mixed surfactant solutions having different $OP(EO)_{10}$ fractions on different plastic surfaces

α	0		0.25		0.50		0.75	
	Exp.	Cal.	Exp.	Cal.	Exp.	Cal.	Exp.	Cal.
HDPE	2.04	2.04	2.25	1.53	1.57	1.02	0.97	0.51
PC	2.26	2.26	2.43	1.69	1.69	1.13	1.22	0.56
PVC	2.85	2.85	2.77	2.14	2.08	1.42	1.31	0.71
ABS	4.02	4.02	3.54	3.01	2.54	2.01	1.52	1.01
PMMA	5.89	5.89	4.78	4.42	3.43	2.94	1.76	1.47
Nylon66	6.36	6.36	5.30	4.77	4.03	3.18	2.20	1.59

Table 4.4 Maximum $OP(EO)_{10}$ adsorption, ($\mu mol/m^2$ of plastic), of mixed surfactant solutions having different $OP(EO)_{10}$ fractions on different plastic surfaces

α	0.25		0.50		0.75		1	
	Exp.	Cal.	Exp.	Cal.	Exp.	Cal.	Exp.	Cal.
HDPE	0.81	1.15	1.59	2.30	3.32	3.45	4.60	4.60
PC	0.82	1.28	1.18	2.56	3.67	3.84	5.12	5.12
PVC	0.87	1.54	1.95	3.08	3.84	4.62	6.16	6.16
ABS	1.16	1.68	2.50	3.35	4.44	5.03	6.71	6.71
PMMA	1.61	1.98	3.36	3.96	5.21	5.95	7.93	7.93
Nylon66	1.77	2.57	3.97	5.15	6.55	7.72	10.30	10.30

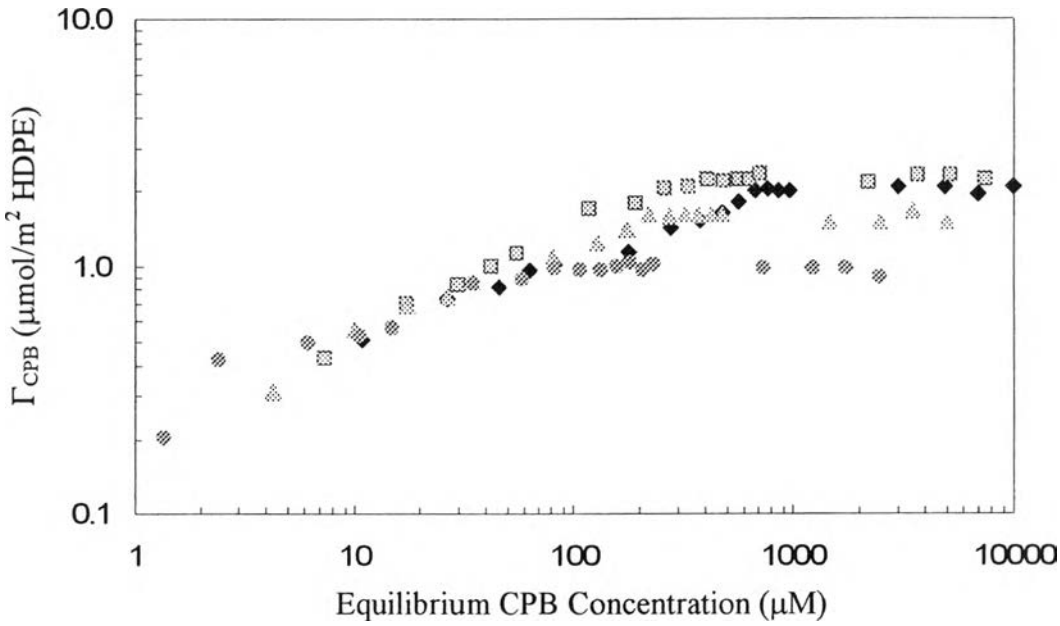

Figure 4.8 Adsorption isotherms of CPB from solution of (♦) CPB, and CPB – $OP(EO)_{10}$ mixtures with α = (■) 0.25, (▲) 0.50, and (●) 0.75 on HDPE.

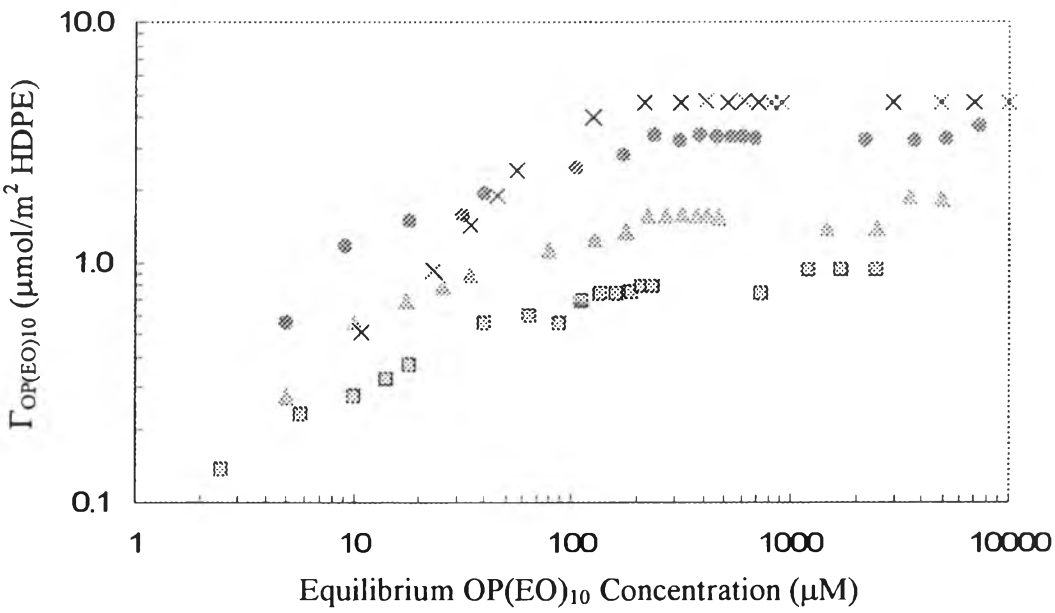

Figure 4.9 Adsorption isotherms of $OP(EO)_{10}$ from solution of (×) $OP(EO)_{10}$, and CPB – $OP(EO)_{10}$ mixtures with α = (■) 0.25, (▲) 0.50, and (●) 0.75 on HDPE.

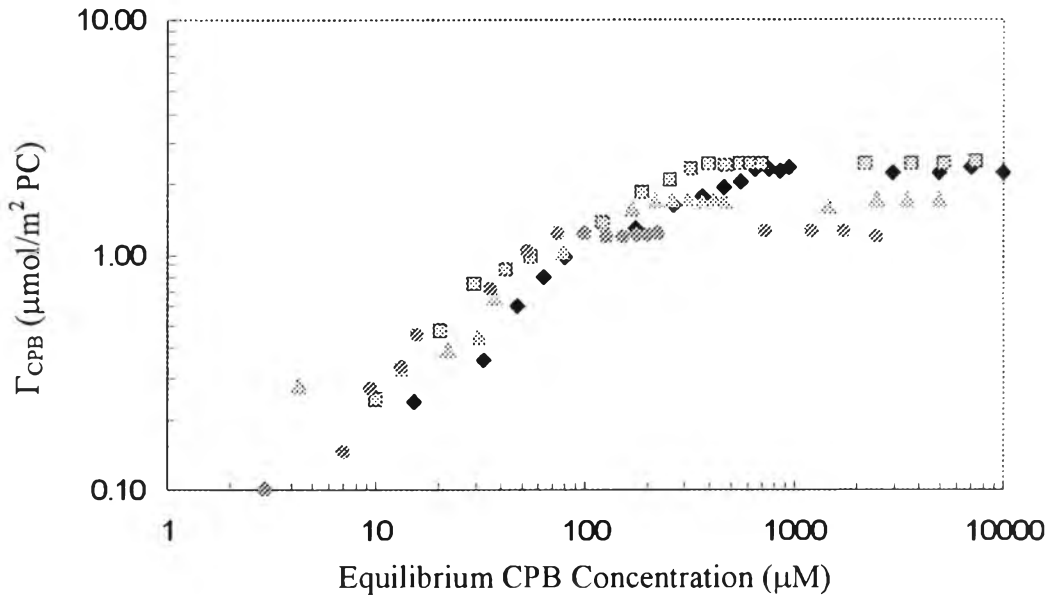

Figure 4.10 Adsorption isotherms of CPB from solution of (♦) CPB, and CPB – $OP(EO)_{10}$ mixtures with α = (■) 0.25, (▲) 0.50, and (●) 0.75 on PC.

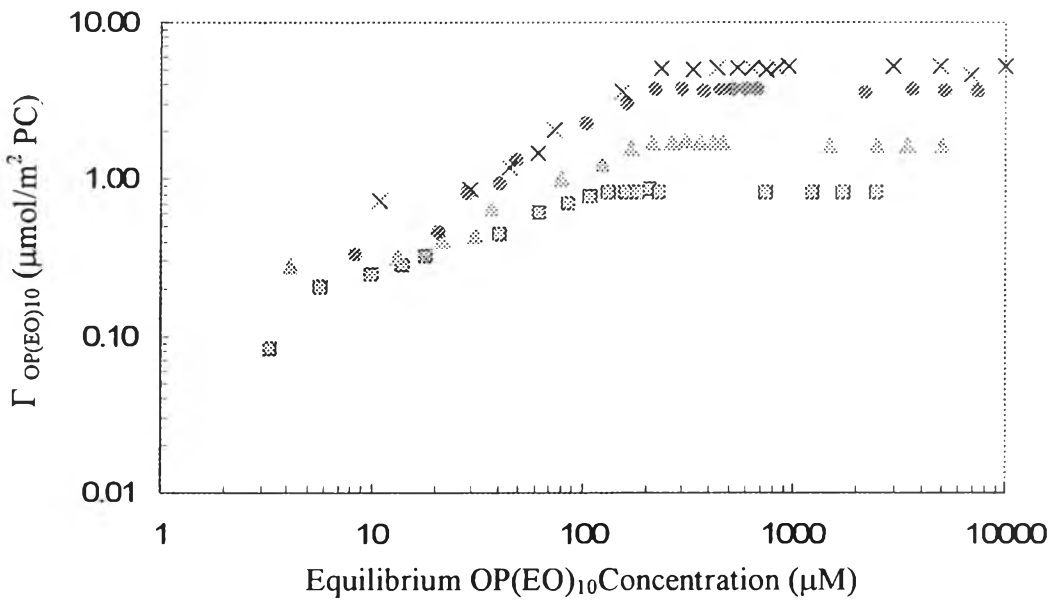

Figure 4.11 Adsorption isotherms of $OP(EO)_{10}$ from solution of (×) $OP(EO)_{10}$, and CPB – $OP(EO)_{10}$ mixtures with α = (■) 0.25, (▲) 0.50, and (●) 0.75 on PC.

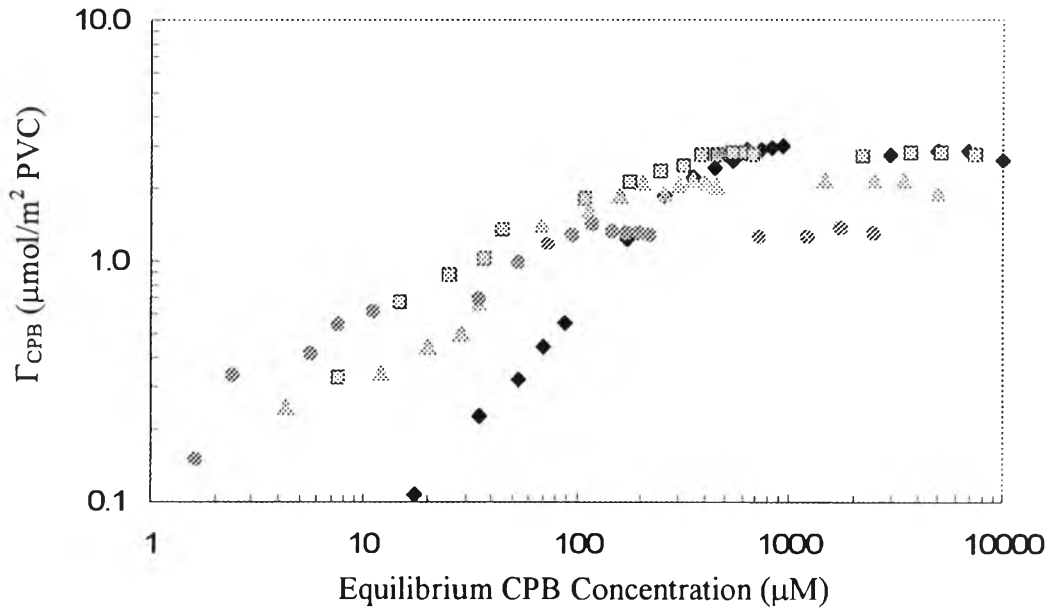

Figure 4.12 Adsorption isotherms of CPB from solution of (♦) CPB, and CPB – $OP(EO)_{10}$ mixtures with α = (■) 0.25, (▲) 0.50, and (●) 0.75 on PVC.

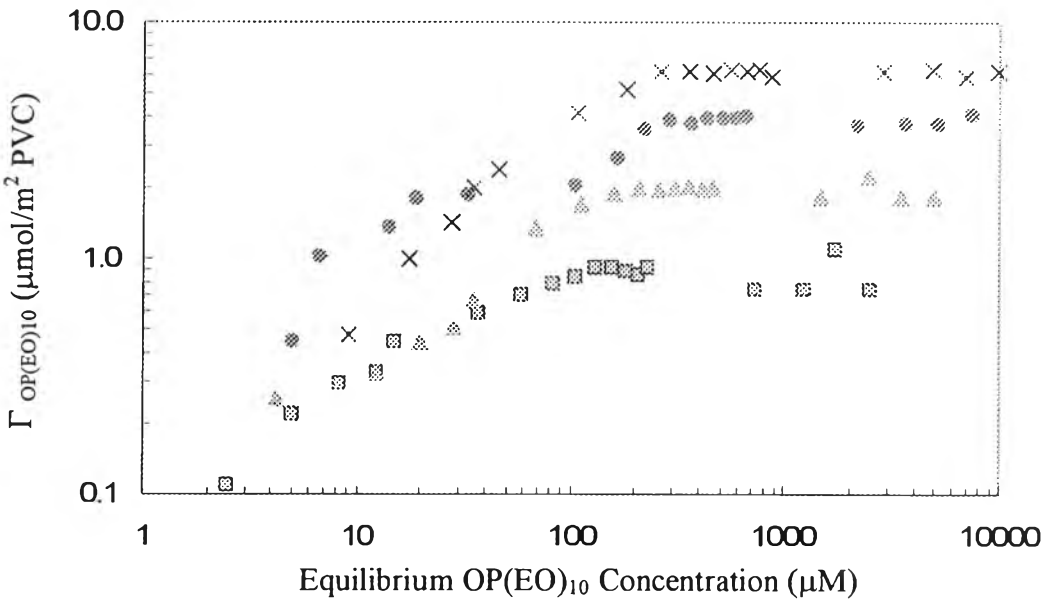

Figure 4.13 Adsorption isotherms of $OP(EO)_{10}$ from solution of (×) $OP(EO)_{10}$, and CPB – $OP(EO)_{10}$ mixtures with α = (■) 0.25, (▲) 0.50, and (●) 0.75 on PVC.

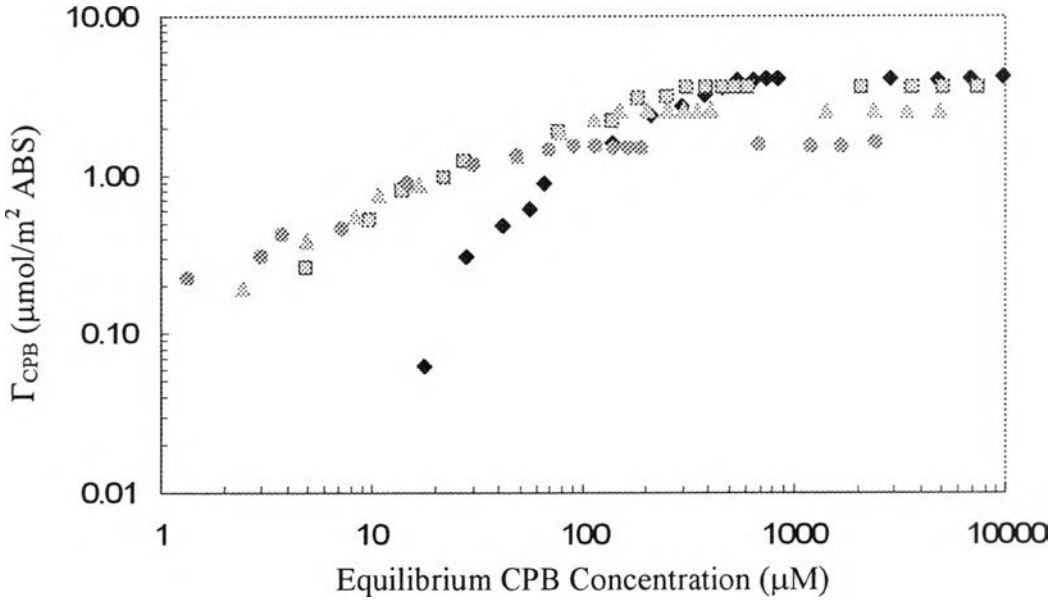

Figure 4.14 Adsorption isotherms of CPB from solution of (♦) CPB, and CPB – $OP(EO)_{10}$ mixtures with α = (■) 0.25, (▲) 0.50, and (●) 0.75 on ABS.

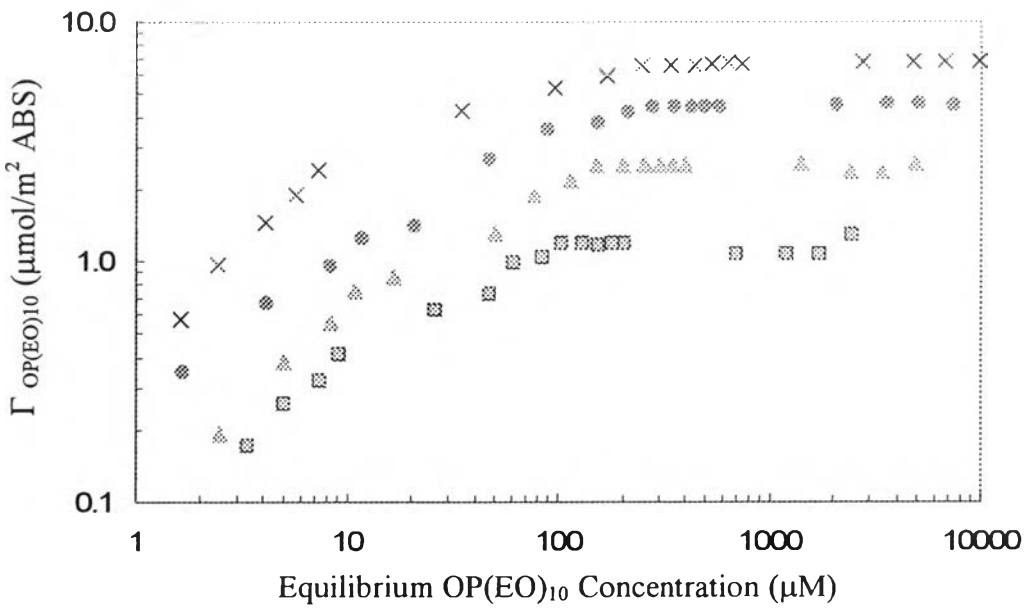

Figure 4.15 Adsorption isotherms of $OP(EO)_{10}$ from solution of (×) $OP(EO)_{10}$, and CPB – $OP(EO)_{10}$ mixtures with α = (■) 0.25, (▲) 0.50, and (●) 0.75 on ABS.

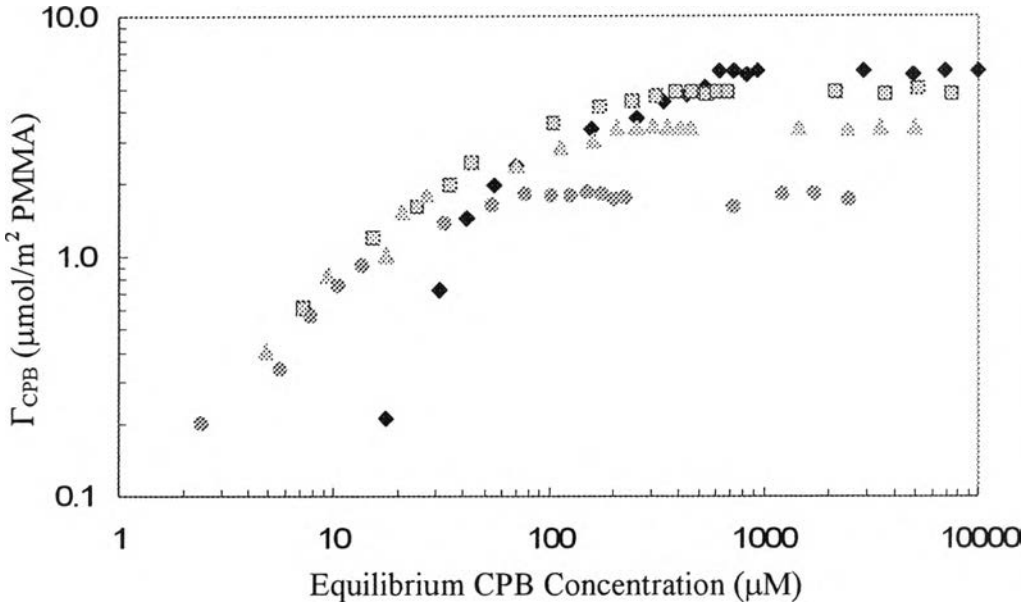

Figure 4.16 Adsorption isotherms of CPB from solution of (♦) CPB, and CPB – $OP(EO)_{10}$ mixtures with α = (■) 0.25, (▲) 0.50, and (●) 0.75 on PMMA.

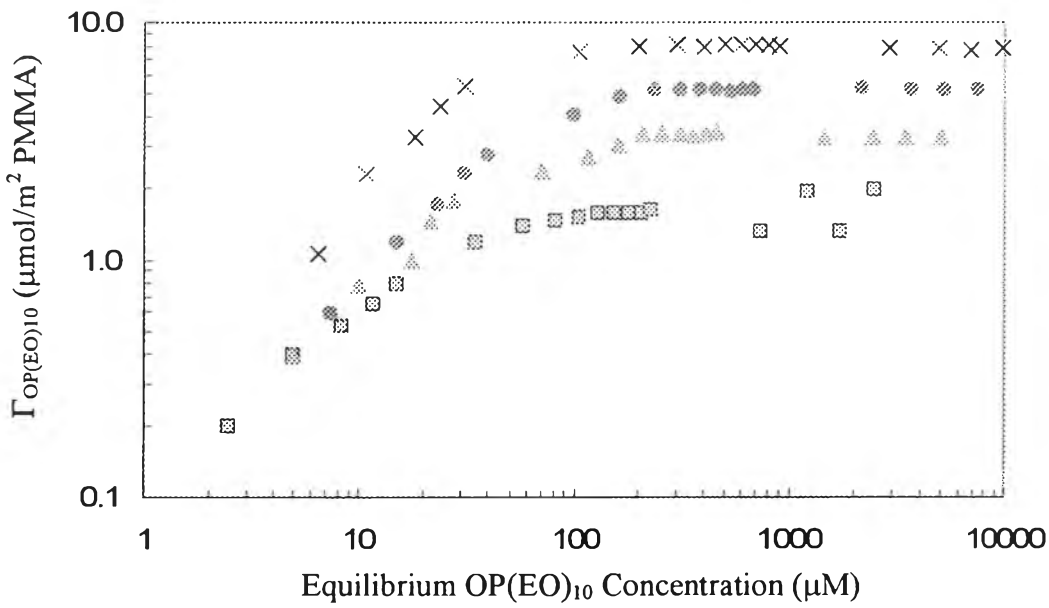

Figure 4.17 Adsorption isotherms of $OP(EO)_{10}$ from solution of (×) $OP(EO)_{10}$, and CPB – $OP(EO)_{10}$ mixtures with α = (■) 0.25, (▲) 0.50, and (●) 0.75 on PMMA.

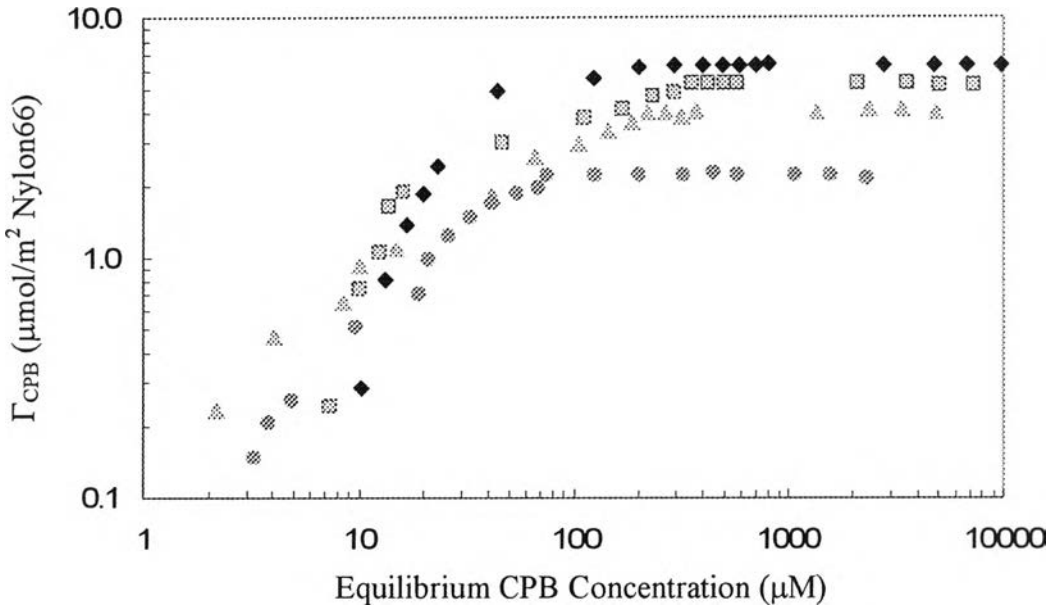

Figure 4.18 Adsorption isotherms of CPB from solution of (♦) CPB, and CPB – $OP(EO)_{10}$ mixtures with α = (■) 0.25, (▲) 0.50, and (●) 0.75 on Nylon66.

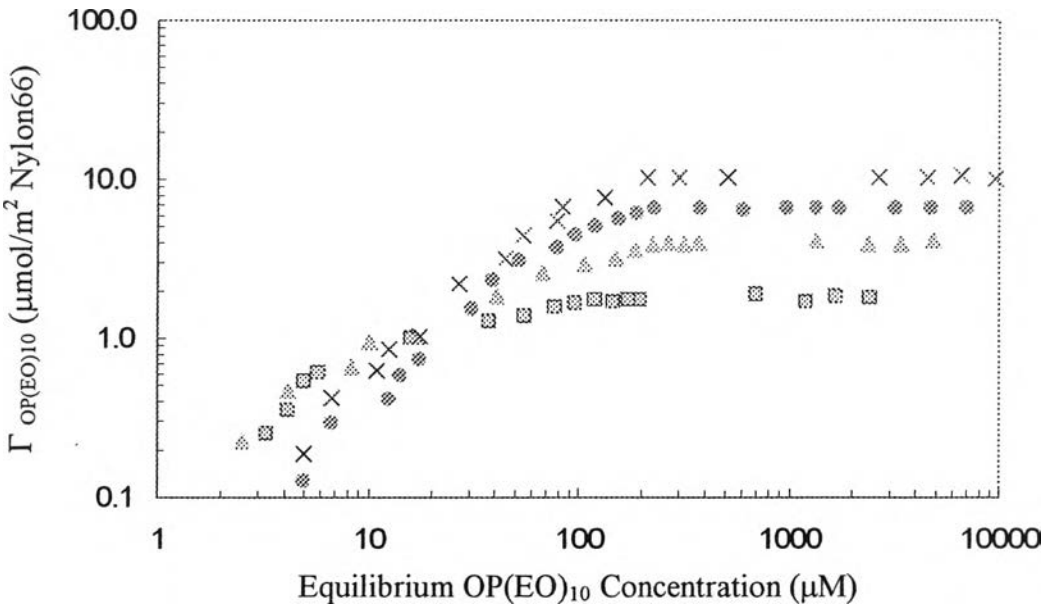

Figure 4.19 Adsorption isotherms of $OP(EO)_{10}$ from solution of (×) $OP(EO)_{10}$, and CPB – $OP(EO)_{10}$ mixtures with α = (■) 0.25, (▲) 0.50, and (●) 0.75 on Nylon66.

4.3.2 Wetting Isotherms for Solution of CPB, $OP(EO)_{10}$, and Their Mixtures on Plastics Surfaces

Contact angle, θ, of the solutions of CPB, $OP(EO)_{10}$, and their mixtures with α was 0.25, 0.50, and 0.75 on HDPE, PC, PVC, ABS, PMMA and Nylon66 are shown in Figure 4.20 – 4.25. For any studied plastic surface, the contact angle decreased significantly with increasing surfactant concentration, and at a very high surfactant concentration, the contact angle remains almost unchanged. Moreover, the wettability on any plastic surface with solutions of $OP(EO)_{10}$ and CPB–$OP(EO)_{10}$ mixtures was much better than that of single CPB solution. $OP(EO)_{10}$ had the highest wetting efficiency, and the wetting efficiency was improved by increasing molar fraction of nonionic surfactant. It means that the combinaiton of CPB and $OP(EO)_{10}$ in a mixture performed a positive effect in the wettability on all studied plastic surfaces (Esumi *et al.*, 1991).

For any surfactant system, the contact angle increased in the following order:

HDPE > PC > PVC > ABS > PMMA > Nylon66

which correlates to the order of the degree of hydrophobicity of plastics, as shown in Table 4.1. It can be concluded that an increase in the polarity of the plastic surfaces increased the wettability of surfactant solutions.

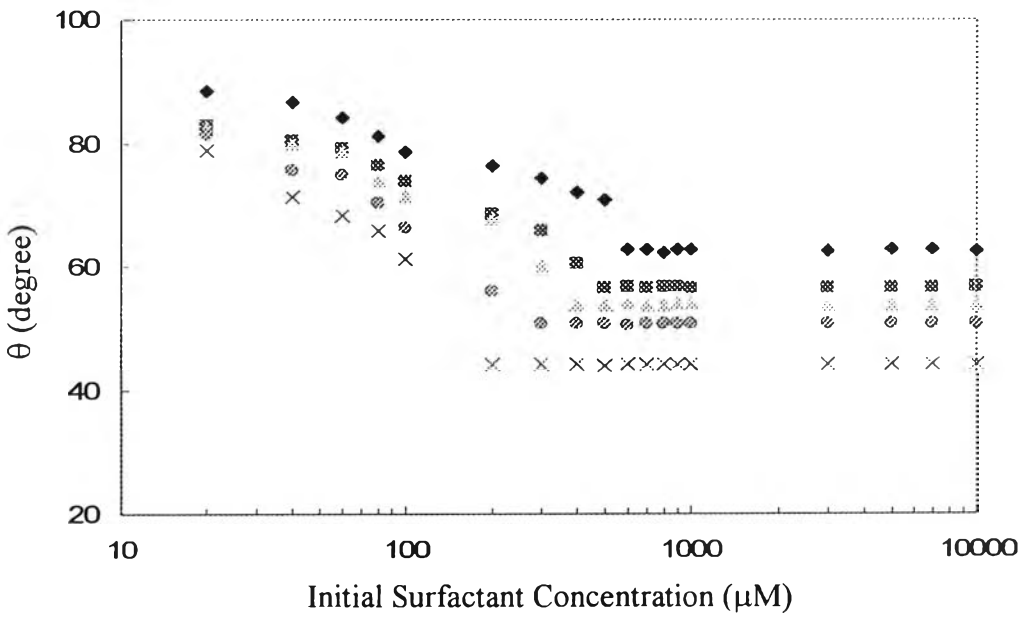

Figure 4.20 Contact angle as a function of surfactant concentration on HDPE for the solutions of (♦) CPB, (×) $OP(EO)_{10}$, and their mixtures with α = (■) 0.25, (▲) 0.50, and (●) 0.75.

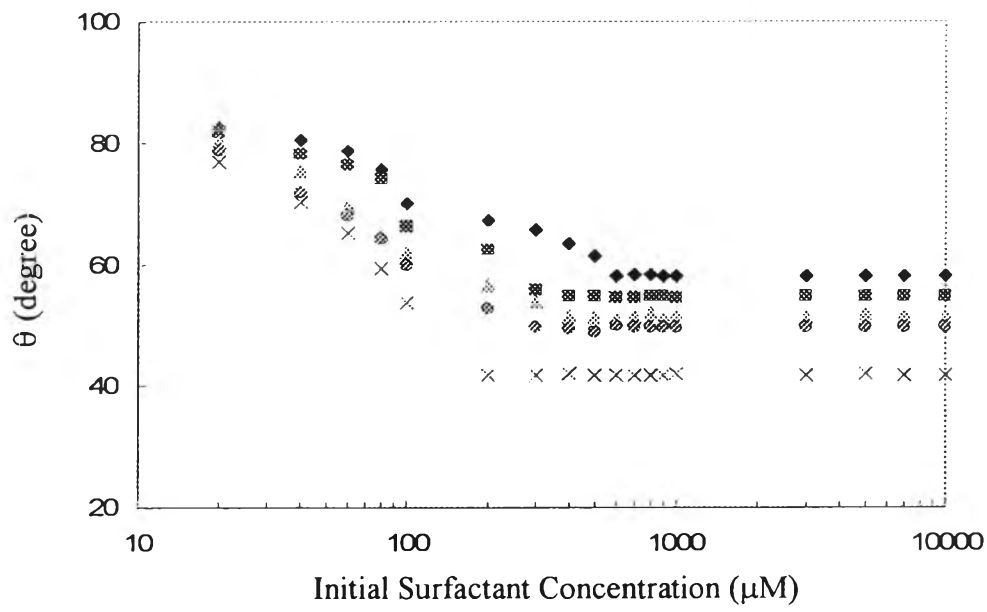

Figure 4.21 Contact angle as a function of surfactant concentration on HDPE for the solutions of (♦) CPB, (×) $OP(EO)_{10}$, and their mixtures with α = (■) 0.25, (▲) 0.50, and (●) 0.75.

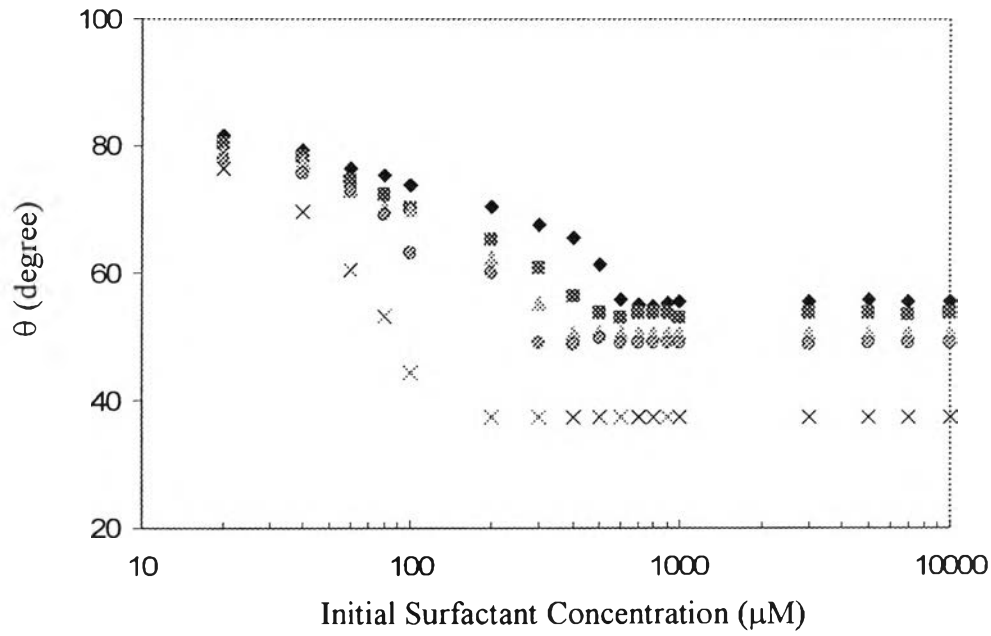

Figure 4.22 Contact angle as a function of surfactant concentration on HDPE for the solutions of (♦) CPB, (×) $OP(EO)_{10}$, and their mixtures with α = (■) 0.25, (▲) 0.50, and (●) 0.75.

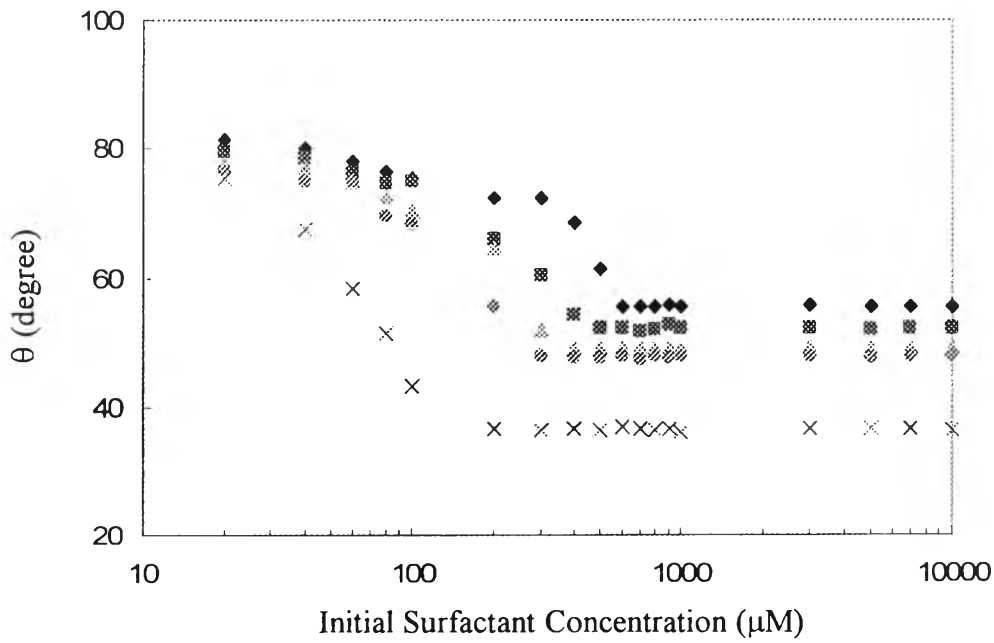

Figure 4.23 Contact angle as a function of surfactant concentration on ABS for the solutions of (♦) CPB, (×) $OP(EO)_{10}$, and their mixtures with α = (■) 0.25, (▲) 0.50, and (●) 0.75.

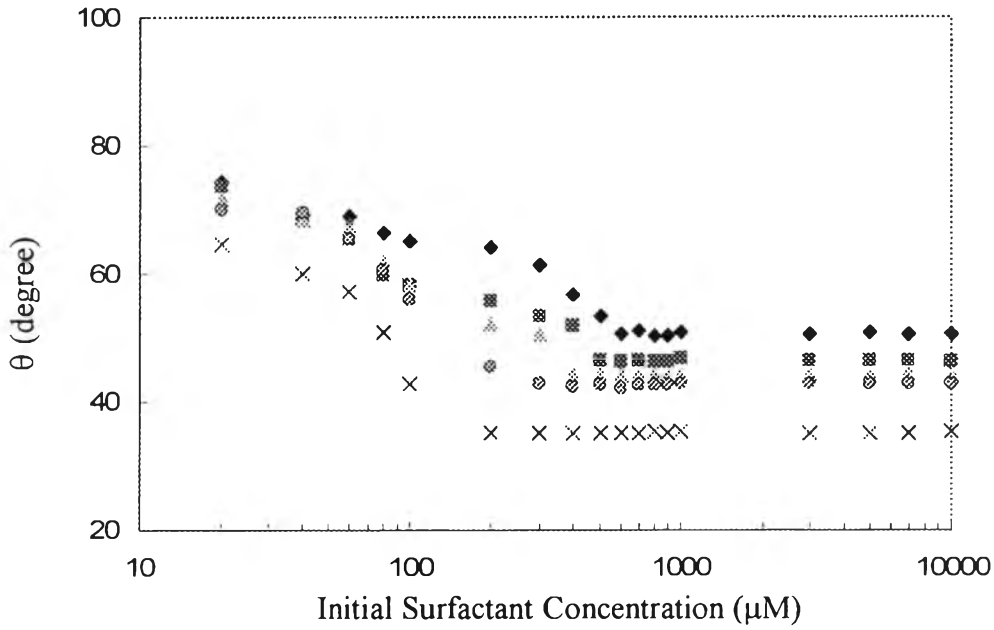

Figure 4.24 Contact angle as a function of surfactant concentration on PMMA for the solutions of (♦) CPB, (×) $OP(EO)_{10}$, and their mixtures with α = (■) 0.25, (▲) 0.50, and (●) 0.75.

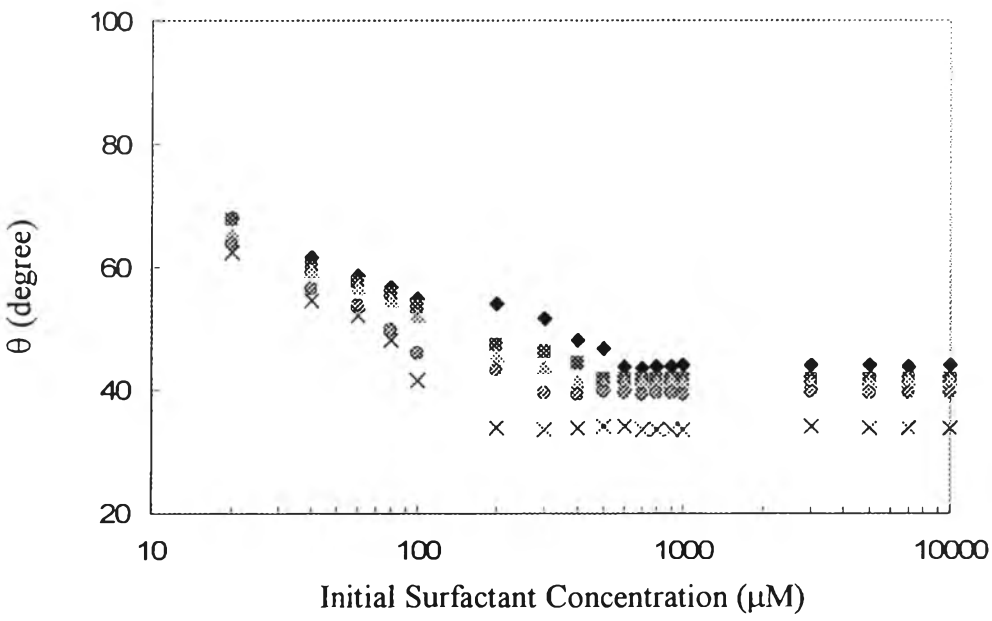

Figure 4.25 Contact angle as a function of surfactant concentration on Nylon66 for the solutions of (♦) CPB, (×) $OP(EO)_{10}$, and their mixtures with α = (■) 0.25, (▲) 0.50, and (●) 0.75.

4.3.3 Wetting Enhancement by Solutions of CPB, $OP(EO)_{10}$, and Their Mixtures

According to Young's equation (see Equation 2.3), that presented the relation between the contact angle and the interfacial tension which was used for studying the wetting behavior of a liquid. Actually, it is quite difficult to measure the γ_{SL} and the γ_{SV} directly. Hence, the term of (γ_{SV} - γ_{SL}) should be considered to understand the wettability of surfactant solution.

If the value of the γ_{SL} and the γ_{SV} were constant, the plot between cosθ and the inversion of the interfacial tension at liquid/vapor interface of surfactant solutions, $1/\gamma_{VL}$, should be linear and intercept at zero. However, Figure 4.26 – 4.31 do not show this relation as they do not intercept at zero.

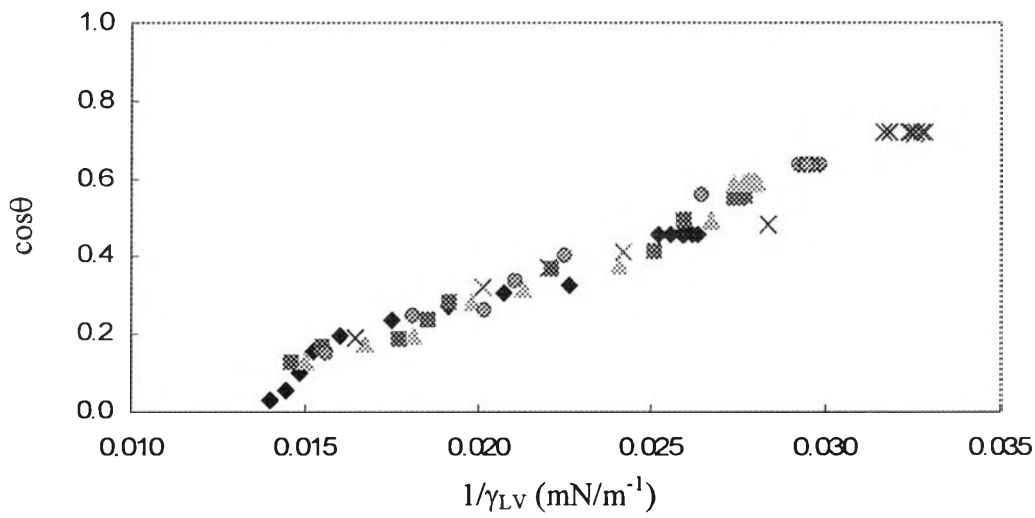

Figure 4.26 Contact angle on HDPE related to inversion of the interfacial tension at liquid vapor interface for solutions of (♦) CPB, (×) $OP(EO)_{10}$, and their mixtures with α = (■) 0.25, (▲) 0.50, and (●) 0.75.

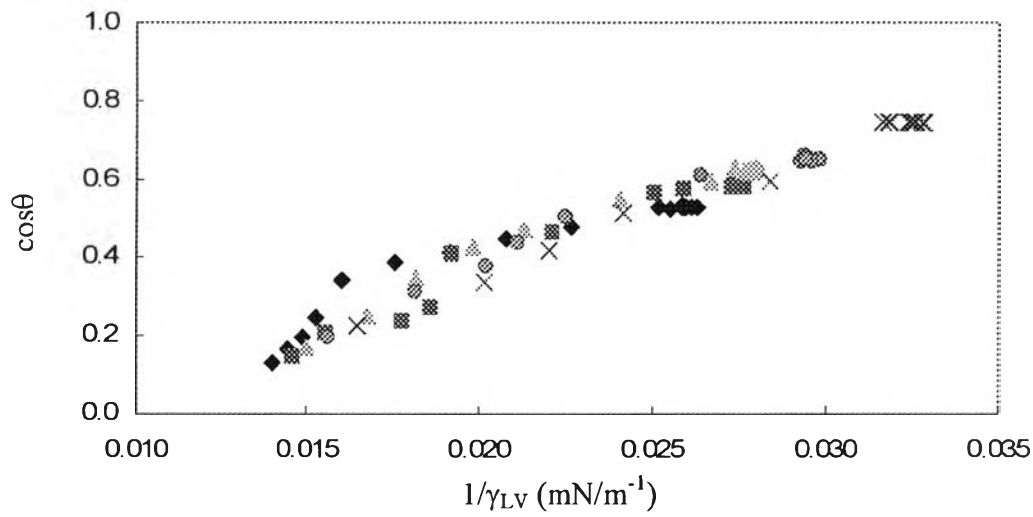

Figure 4.27 Contact angle on PC related to inversion of the interfacial tension at liquid vapor interface for solutions of (♦) CPB, (×) $OP(EO)_{10}$, and their mixtures with α = (■) 0.25, (▲) 0.50, and (●) 0.75.

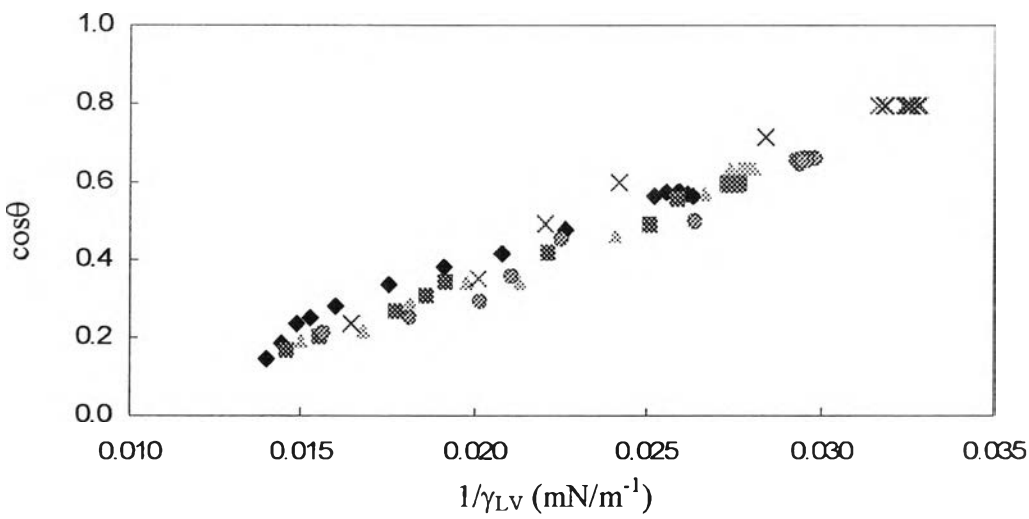

Figure 4.28 Contact angle on PVC related to inversion of the interfacial tension at liquid vapor interface for solutions of (♦) CPB, (×) $OP(EO)_{10}$, and their mixtures with α = (■) 0.25, (▲) 0.50, and (●) 0.75.

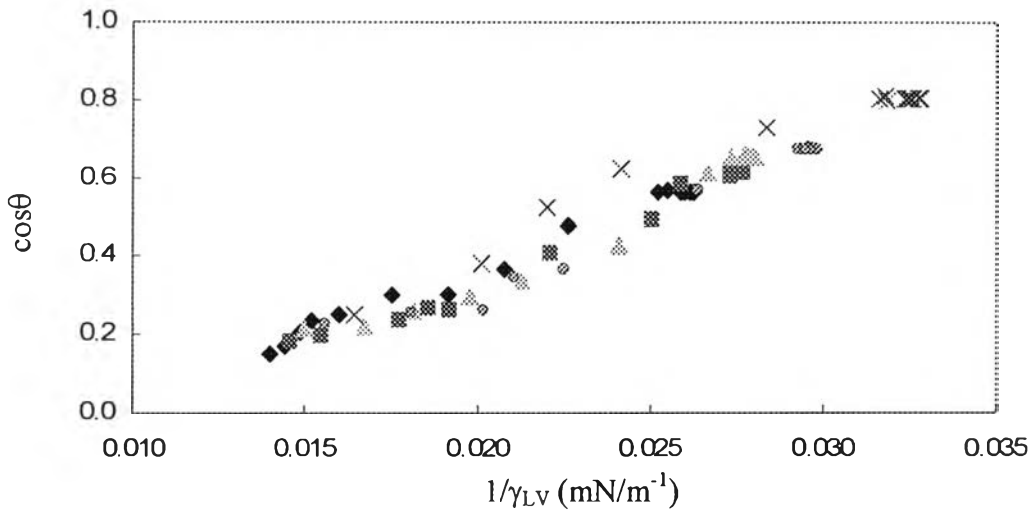

Figure 4.29 Contact angle on ABS related to inversion of the interfacial tension at liquid vapor interface for solutions of (♦) CPB, (×) $OP(EO)_{10}$, and their mixtures with α = (■) 0.25, (▲) 0.50, and (●) 0.75.

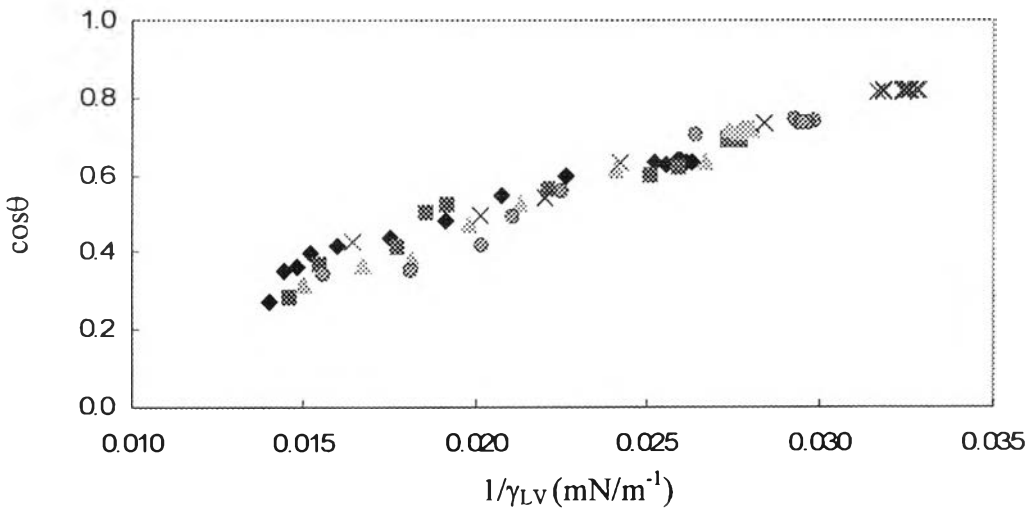

Figure 4.30 Contact angle on PMMA related to inversion of the interfacial tension at liquid vapor interface for solutions of (♦) CPB, (×) $OP(EO)_{10}$, and their mixtures with α = (■) 0.25, (▲) 0.50, and (●) 0.75.

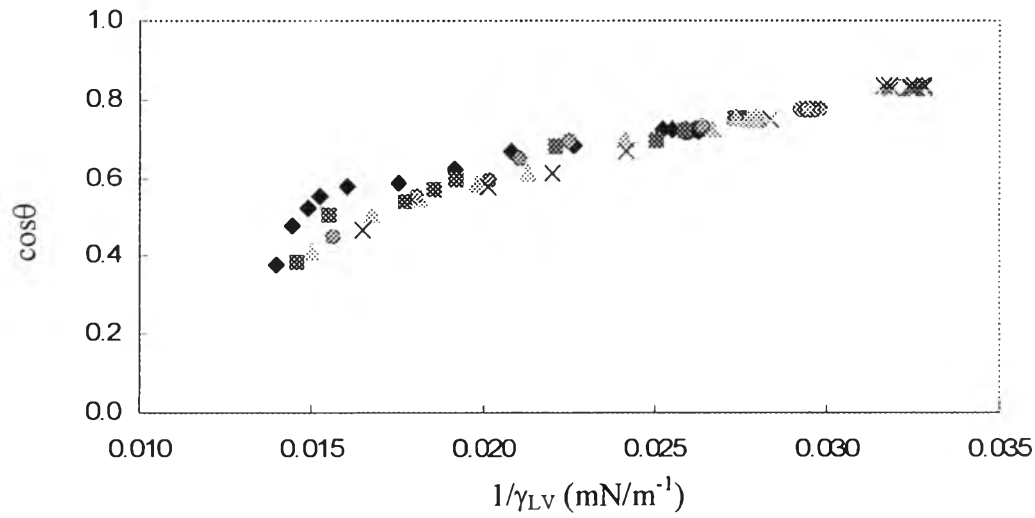

Figure 4.31 Contact angle on Nylon66 related to inversion of the interfacial tension at liquid vapor interface for solutions of (♦) CPB, (×) $OP(EO)_{10}$, and their mixtures with α = (■) 0.25, (▲) 0.50, and (●) 0.75.

Another possible way to examine the variation of the (γ_{SV} - γ_{SL}) term is to take a look at the product of cosθ multiply with γ_{LV} (or γ_{LV}cosθ). From Equation 2.3, if γ_{LV}cosθ was constant, the value of (γ_{SV} - γ_{SL}) would be constant. As shown in Figure 4.32 – 4.37, the value of (γ_{SV} - γ_{SL}) varied with surfactant concentration in the region of concentration lower the CMC but it was nearly constant after the CMC point.

Generally, the γ_{SV} could be assumed to be independent of the surfactant concentration since the dry solid had not been contacted by the solution yet and the transfer of the non-volatile surfactants to the solid/vapor interface during measuring contact angle via vapor phase seemed unlikely (Gau and Zografi, 1990). This indicated that the γ_{SL} varied with surfactant concentration in case of both of the single surfactant system and the mixed surfactant system in the region of concentration lower the CMC but it remained almost unchanged after the CMC point.

However, for Nylon66 and any surfactant system, the value of γ_{LV}cosθ first increased, reached their maximum values, and then decreased before

being nearly constant at about the CMC. At low surfactant concentration, the ascending part of the isotherm was influenced by increasing the value of cosθ. For higher surfactant concentration, a decrease in the surface tension had effect over the increase in the value of cosθ, resulted in the reduction of the value of $\gamma_{LV}\cos\theta$ before reaching the plateau.

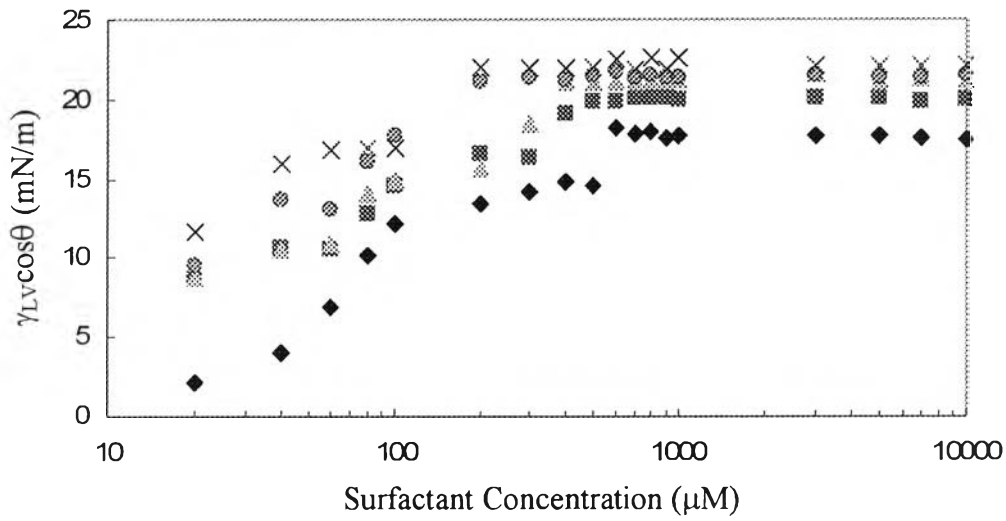

Figure 4.32 $\gamma_{LV}\cos\theta$ on HDPE related to total surfactant concentration for solutions of (♦) CPB, (×) $OP(EO)_{10}$, and their mixtures with α = (■) 0.25, (▲) 0.50, and (●) 0.75.

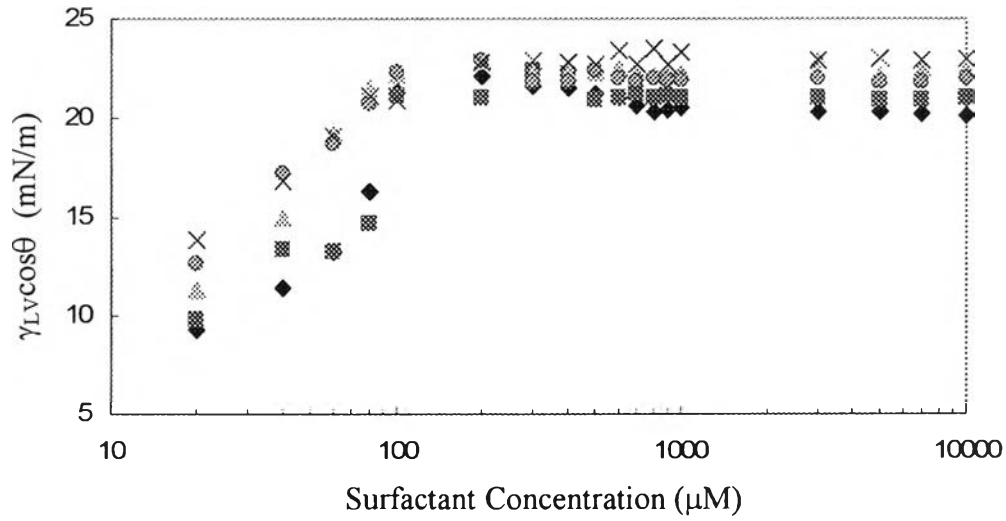

Figure 4.33 $\gamma_{LV}\cos\theta$ on PC related to total surfactant concentration for solutions of (♦) CPB, (×) $OP(EO)_{10}$, and their mixtures with α = (■) 0.25, (▲) 0.50, and (●) 0.75.

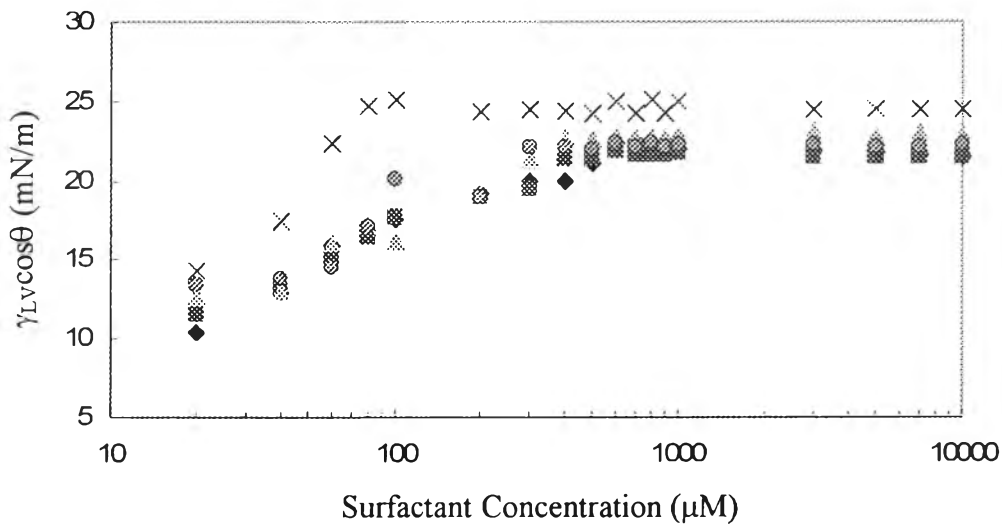

Figure 4.34 $\gamma_{LV}\cos\theta$ on PVC related to total surfactant concentration for solutions of (♦) CPB, (×) $OP(EO)_{10}$, and their mixtures with α = (■) 0.25, (▲) 0.50, and (●) 0.75.

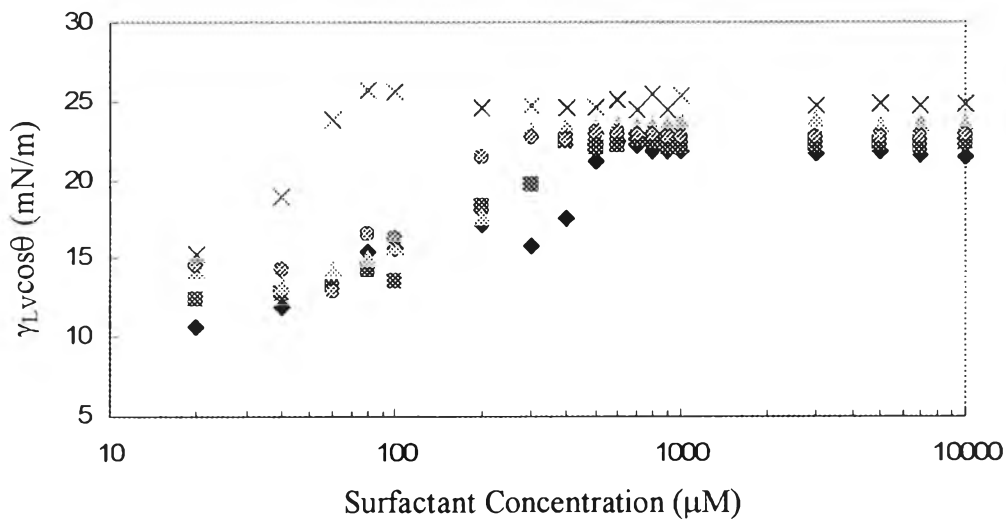

Figure 4.35 $\gamma_{LV}\cos\theta$ on ABS related to total surfactant concentration for solutions of (♦) CPB, (×) $OP(EO)_{10}$, and their mixtures with α = (■) 0.25, (▲) 0.50, and (●) 0.75.

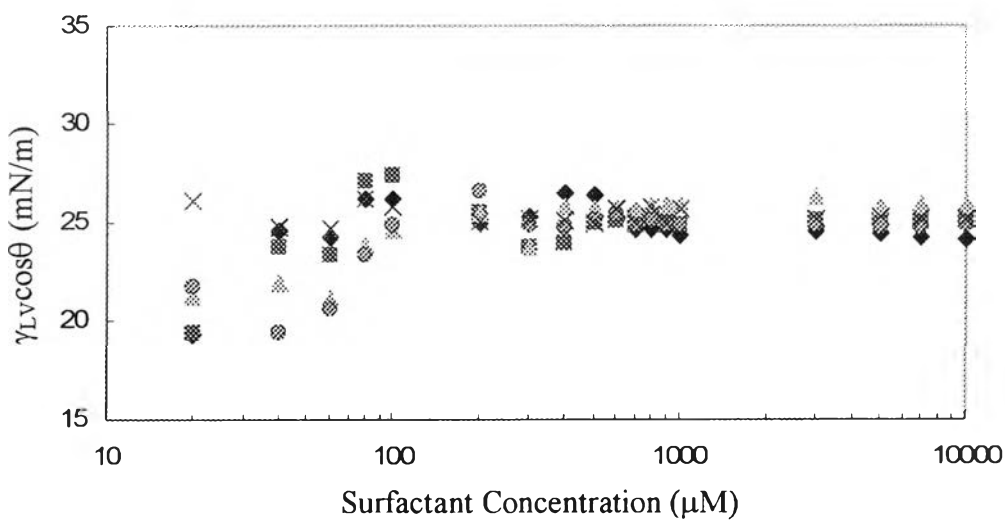

Figure 4.36 $\gamma_{LV}\cos\theta$ on PMMA related to total surfactant concentration for solutions of (♦) CPB, (×) $OP(EO)_{10}$, and their mixtures with α = (■) 0.25, (▲) 0.50, and (●) 0.75.

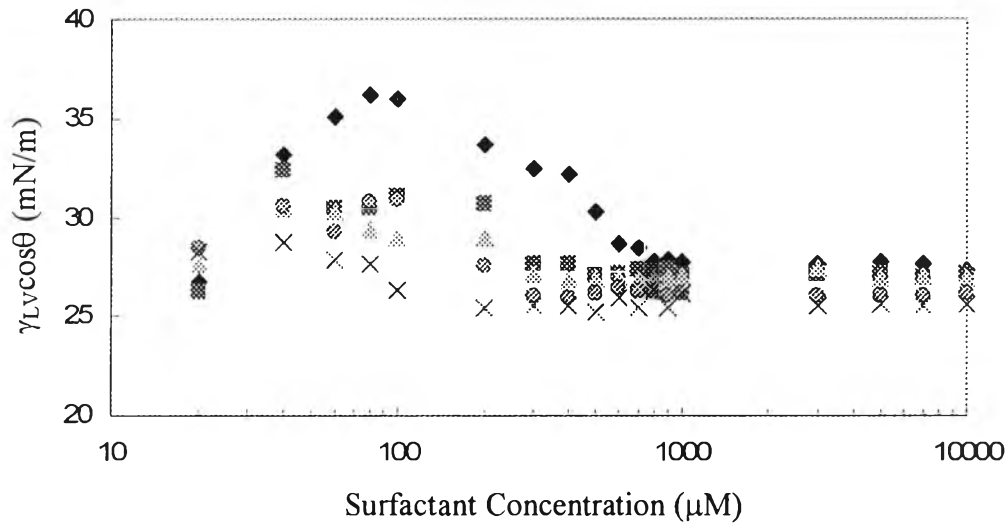

Figure 4.37 $\gamma_{LV}\cos\theta$ on Nylon66 related to total surfactant concentration for solutions of (♦) CPB, (×) $OP(EO)_{10}$, and their mixtures with α = (■) 0.25, (▲) 0.50, and (●) 0.75.

Actually we could not measure the γ_{SL} directly but there was an other possible way to examine the variation of the γ_{SL} is to calculate the γ_{SL} at concentration c, $\gamma_{SL}(c)$, related to the γ_{SL} at reference state which had no surfactant or in pure water, $\gamma_{SL}(w)$, using the contact angle and the interfacial tension at the liquid/vapor interface data. Equation 2.3 might be written as

$$\gamma_{LV}(w)\cos\theta(w) - \gamma_{LV}(c)\cos\theta(c) = [\gamma_{SV}(w) - \gamma_{SL}(w)] - [\gamma_{SV}(c) - \gamma_{SL}(c)]$$
$$= \gamma_{SL}(c) - \gamma_{SL}(w), \qquad (4.2)$$

where (w) refers to the standard state when no surfactant presents and (c) refers to the properties of the surfactant solution at concentration c.

Figure 4.38 - 4.43 indicated the correlation between the relative interfacial tension, $\gamma_{SL}(c) - \gamma_{SL}(w)$, and surfactant concentration. If the $\gamma_{SL}(w)$ was commonly assumed to be constant, these plots would provide the relation between $\gamma_{SL}(c)$ and surfactant concentration. For any non polar plastic surface, the $\gamma_{SL}(c)$ decreased when the surfactant concentration rose and it also decreased with increasing the molar fraction of nonionic surfactant in mixtures. When plastic

surfaces became more polar, the $\gamma_{SL}(c)$ decreased insignificantly and tended to increase when the molar fraction of nonionic surfactant in mixtures increased.

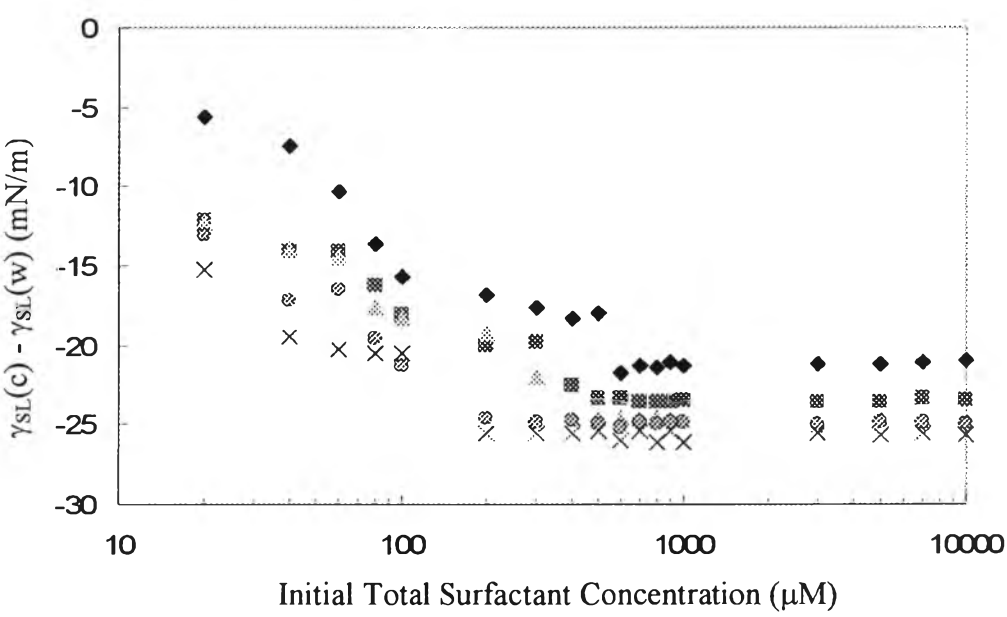

Figure 4.38 Relative interfacial tension at solid/liquid interface of HDPE as a function of concentration of solutions of (♦) CPB, (×) $OP(EO)_{10}$, and their mixtures with α = (■) 0.25, (▲) 0.50, and (●) 0.75.

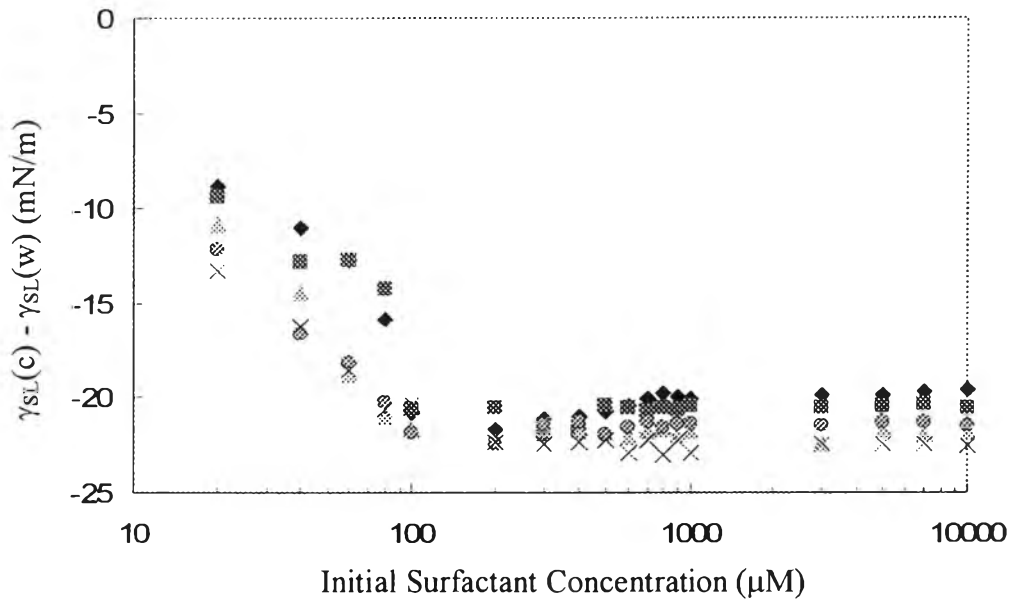

Figure 4.39 Relative interfacial tension at solid/liquid interface of PC as a function of concentration of solutions of (♦) CPB, (×) $OP(EO)_{10}$, and their mixtures with α = (■) 0.25, (▲) 0.50, and (●) 0.75.

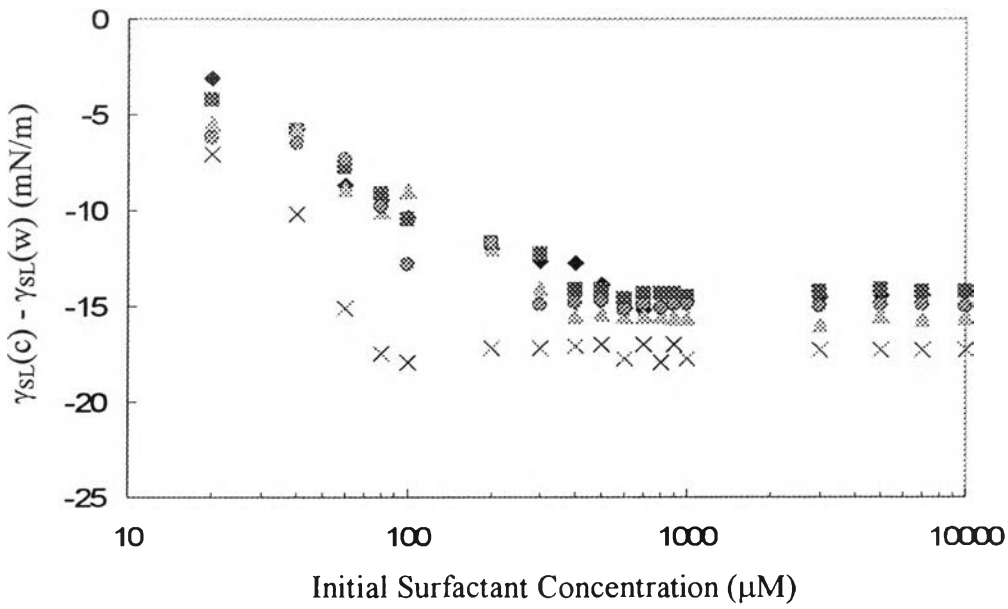

Figure 4.40 Relative interfacial tension at solid/liquid interface of PVC as a function of concentration of solutions of (♦) CPB, (×) $OP(EO)_{10}$, and their mixtures with α = (■) 0.25, (▲) 0.50, and (●) 0.75.

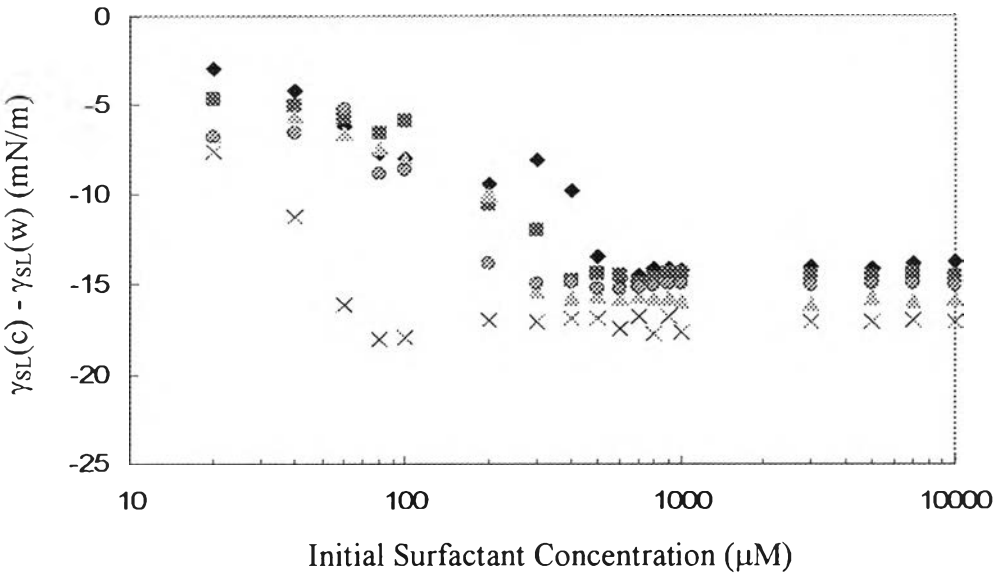

Figure 4.41 Relative interfacial tension at solid/liquid interface of ABS as a function of concentration of solutions of (♦) CPB, (×) $OP(EO)_{10}$, and their mixtures with α = (■) 0.25, (▲) 0.50, and (●) 0.75.

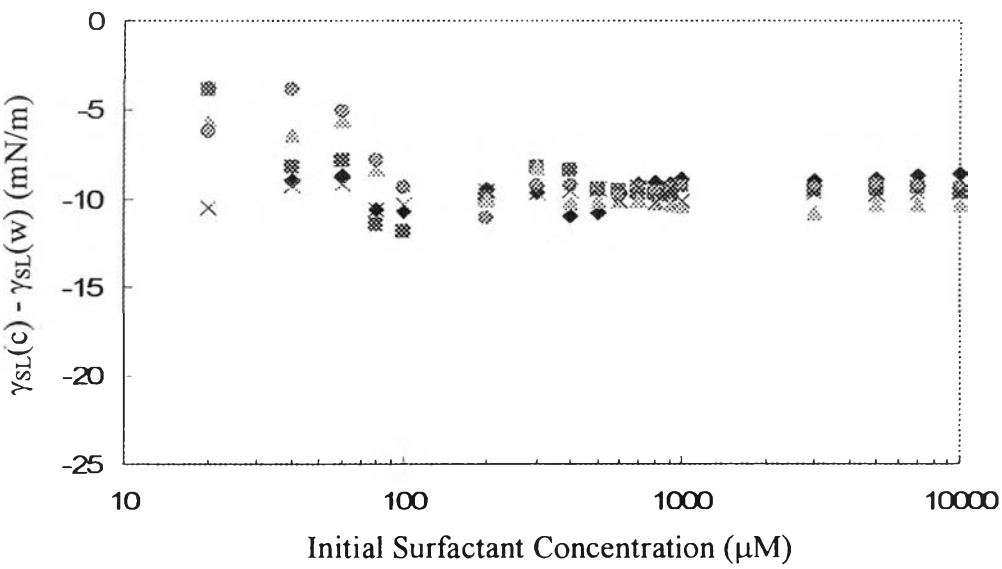

Figure 4.42 Relative interfacial tension at solid/liquid interface of PMMA as a function of concentration of solutions of (♦) CPB, (×) $OP(EO)_{10}$, and their mixtures with α = (■) 0.25, (▲) 0.50, and (●) 0.75.

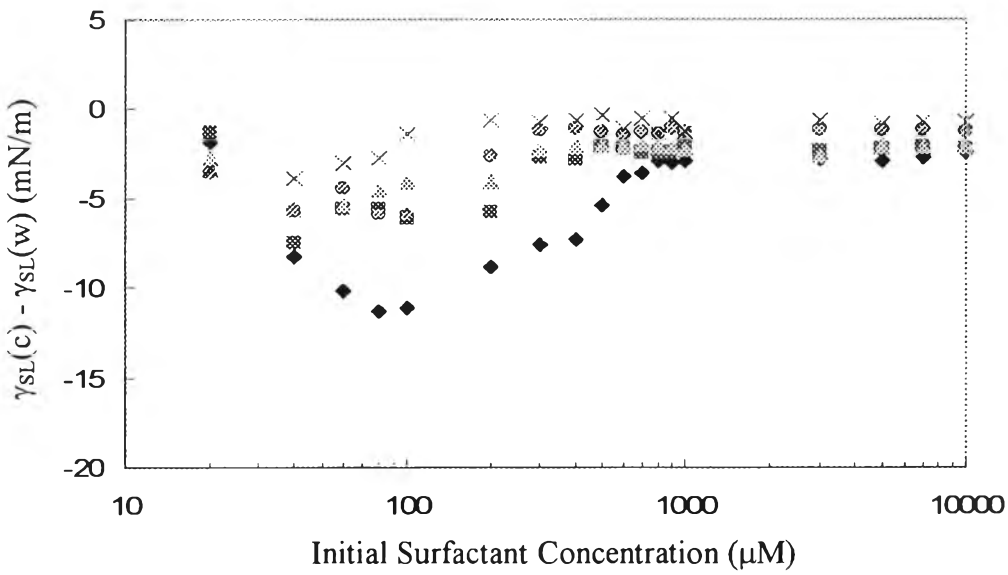

Figure 4.43 Relative interfacial tension at solid/liquid interface of Nylon66 as a function of concentration of solutions of (♦) CPB, (×) $OP(EO)_{10}$, and their mixtures with α = (■) 0.25, (▲) 0.50, and (●) 0.75.

This relative interfacial tension at the solid/liquid interface could be related with total amount of adsorbed surfactant as shown in Figure 4.44 - 4.49. For low polar plastic, the increase in surfactant adsorption caused the γ_{SL} reduction, which resulted in the contact angle reduction. Hence, the changes in contact angles induced by surfactant attributed not only to the changes in the γ_{LV} but it also could attribute to the changes the γ_{SL}. Moreover, the increase in molar fraction of nonionic surfactant could reduce the γ_{SL} more.

However, for higher polar plastic surfaces, in case of Nylon66, the γ_{SL} reduction was insignificantly affected by increasing surfactant adsorption. The γ_{SL} increased with increasing the nonionic surfactant molar fraction. It means that the increase in surfactant adsorption and the addition of $OP(EO)_{10}$ into the CPB solution had less effect on the γ_{SL} reduction than on the γ_{LV} reduction. An increasing in the γ_{SL} on Nylon66 surface was attributed to the adsorption tendency of surfactant molecules at the liquid/vapor interface, as shown in adhesion tension plot on Nylon66 (see Figure 4.55).

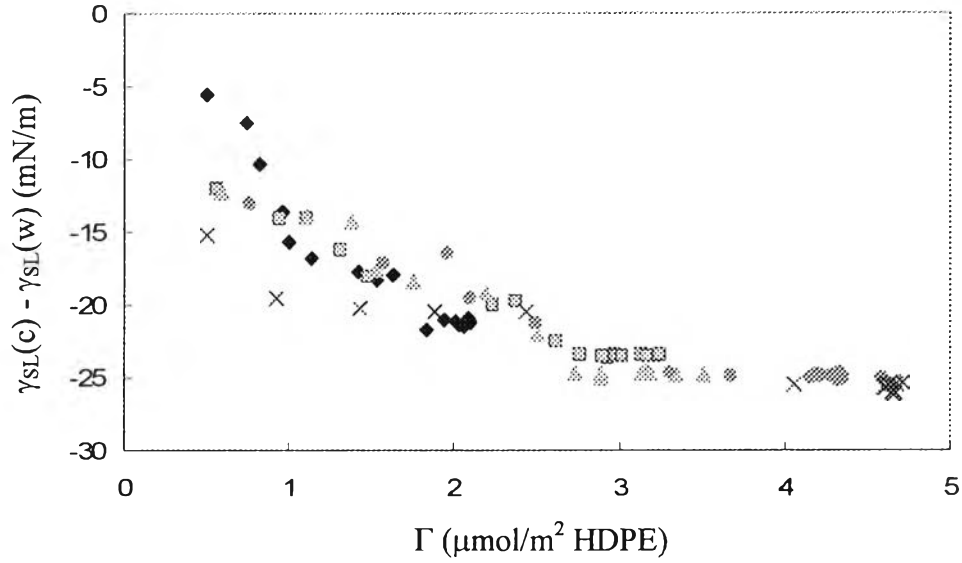

Figure 4.44 Relative interfacial tension at solid/liquid interface of HDPE as a function of adsorption of solutions of (♦) CPB, (×) $OP(EO)_{10}$, and their mixtures with α = (■) 0.25, (▲) 0.50, and (●) 0.75.

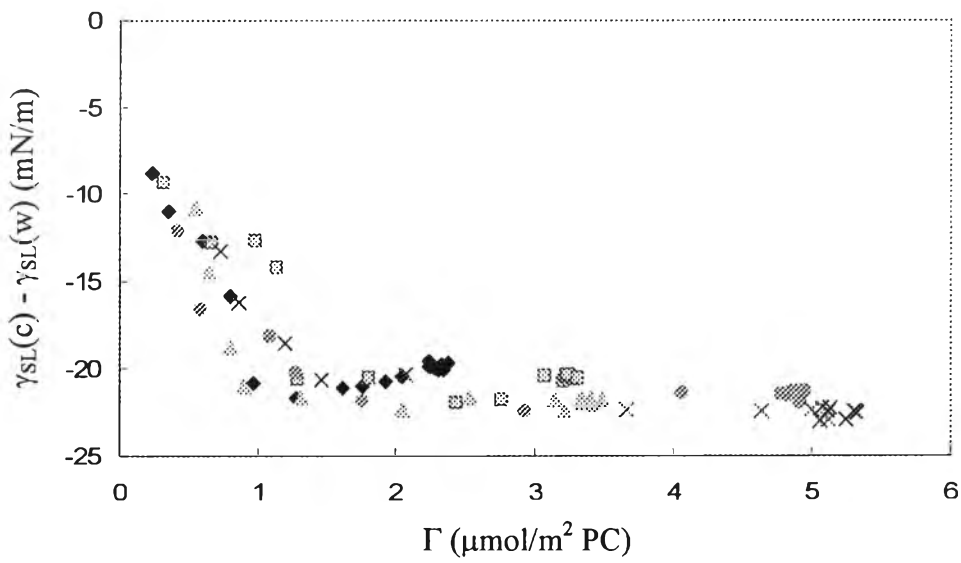

Figure 4.45 Relative interfacial tension at solid/liquid interface of PC as a function of adsorption of solutions of (♦) CPB, (×) $OP(EO)_{10}$, and their mixtures with α = (■) 0.25, (▲) 0.50, and (●) 0.75.

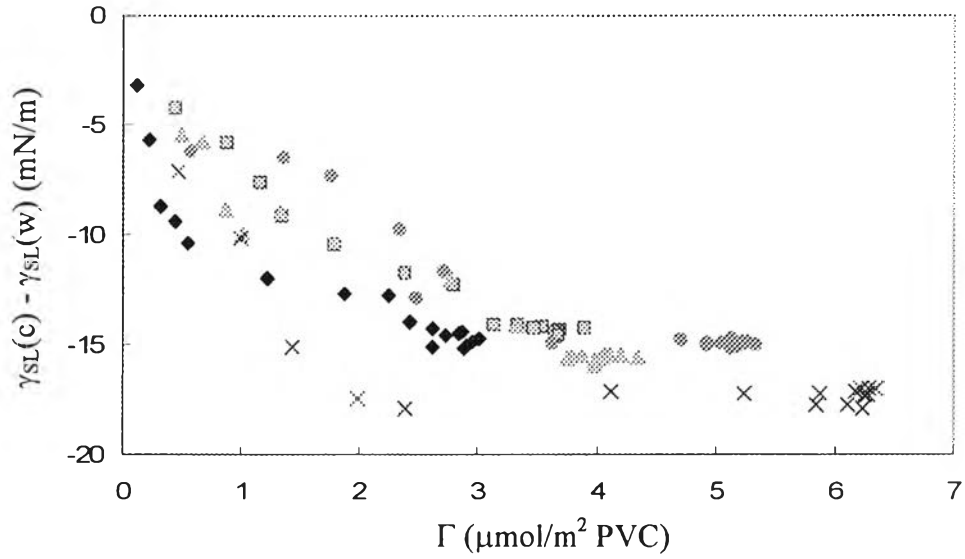

Figure 4.46 Relative interfacial tension at solid/liquid interface of PVC as a function of adsorption of solutions of (♦) CPB, (×) $OP(EO)_{10}$, and their mixtures with α = (■) 0.25, (▲) 0.50, and (●) 0.75.

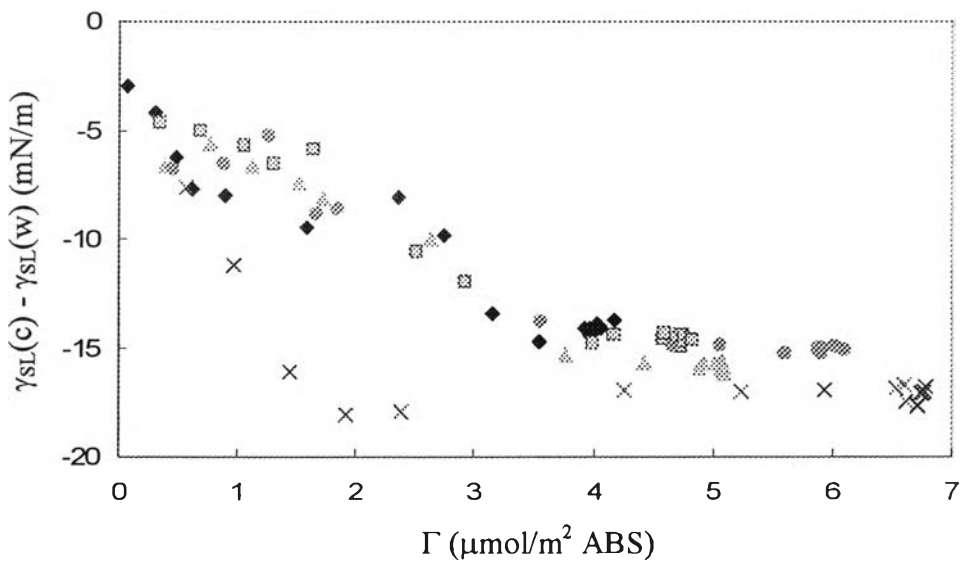

Figure 4.47 Relative interfacial tension at solid/liquid interface of ABS as a function of adsorption of solutions of (♦) CPB, (×) $OP(EO)_{10}$, and their mixtures with α = (■) 0.25, (▲) 0.50, and (●) 0.75.

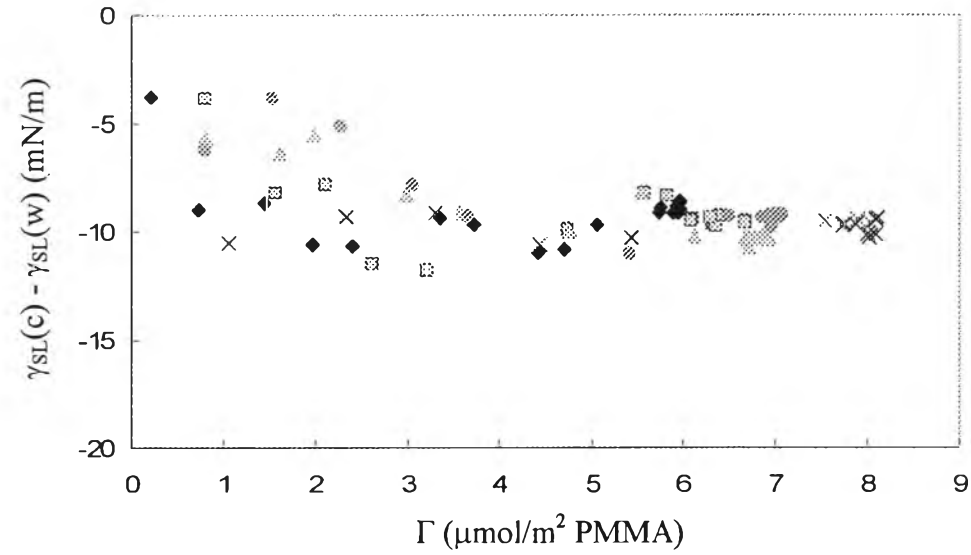

Figure 4.48 Relative interfacial tension at solid/liquid interface of PMMA as a function of adsorption of solutions of (♦) CPB, (×) $OP(EO)_{10}$, and their mixtures with α = (■) 0.25, (▲) 0.50, and (●) 0.75.

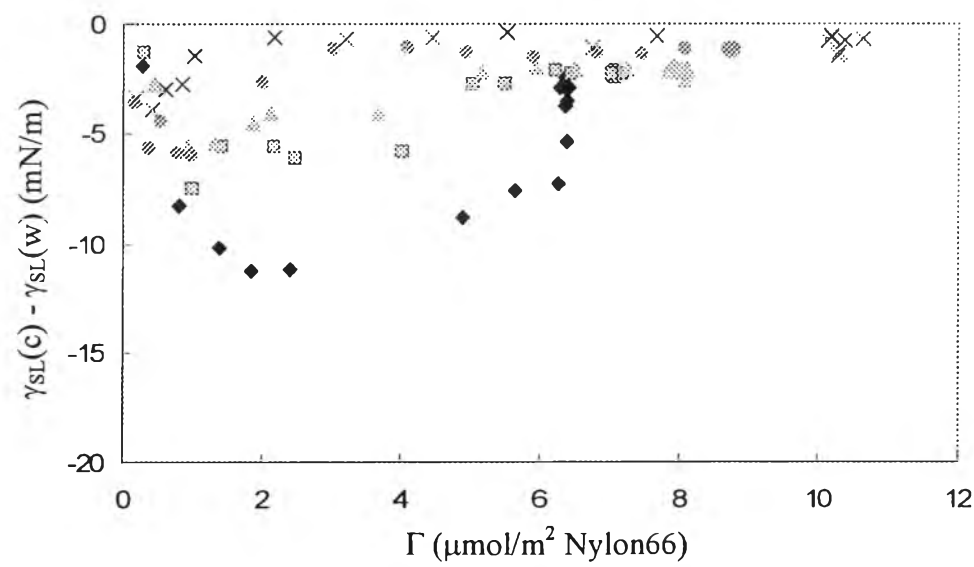

Figure 4.49 Relative interfacial tension at solid/liquid interface of Nylon66 as a function of adsorption of solutions of (♦) CPB, (×) $OP(EO)_{10}$, and their mixtures with α = (■) 0.25, (▲) 0.50, and (●) 0.75.

The relation of adsorption to equilibrium wetting could be investigated by combining the Gibbs adsorption equation with Young's equation yields as shown in Equation 2.4, was called adhesion tension plots, of $\gamma_{LV}\cos\theta$ versus γ_{LV}. If surface excess concentration at the solid/vapor interface, Γ_{SV}, was assumed to be negligible, the slope of adhesion tension plot should be the ratio of surface excess concentration at the solid/liquid to the liquid/vapor interface, Γ_{SL}/Γ_{LV}, as depicted in Figure 4.50 - 4.55.

These adhesion tension profiles gave negative slopes but they were still less than zero; $-1<\text{slope}<0$, indicating higher surfactant adsorption at the liquid/vapor than at the solid/liquid interface; $\Gamma_{SL}<\Gamma_{LV}$. It could be also seen in these figures that the slopes were being less negative which indicated that surfactant molecules tended to adsorb at the liquid/vapor interface more than that at the solid/liquid interface as the adsorbed surface became more polar. Furthermore, the addition of nonionic surfactant did not show significantly effect on this. These results also correlated to the reduction of the γ_{LV} and the γ_{SL} (see Figure 4.44 - 4.49). However, the adhesion tension on Nylon66 decreased gradually when the surface tension decreased, signifying the importance of surfactant adsorption at the solid/vapor interface. For good wetting and strong adhesion forces, the γ_{LV} must be smaller than the γ_{SV}. Besides, a decrease in the adhesion tension profiles means the liquid molecules have a stronger attraction to the solid surface than each other (Özdemir *et al.*, 2004).

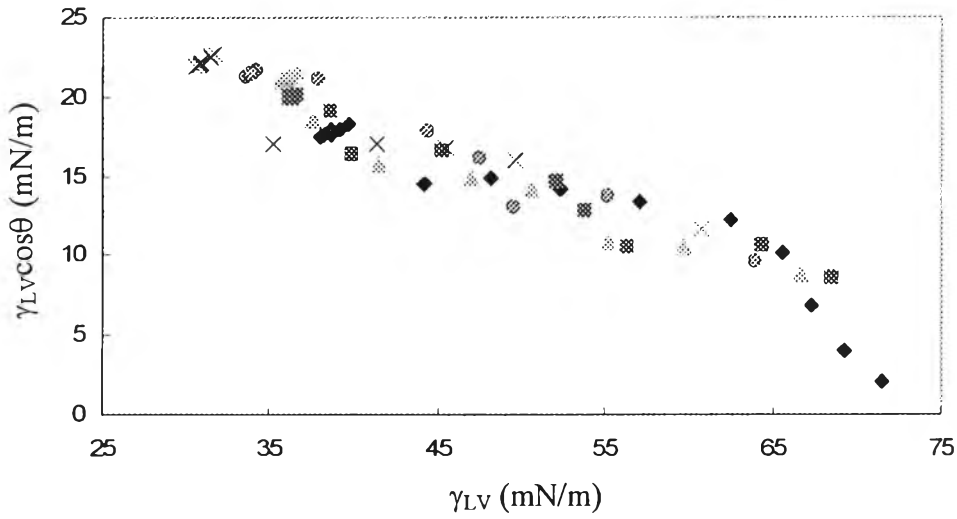

Figure 4.50 Adhesion tension plot for solutions of (♦) CPB, (×) $OP(EO)_{10}$, and their mixtures with α = (■) 0.25, (▲) 0.50, and (●) 0.75 on HDPE.

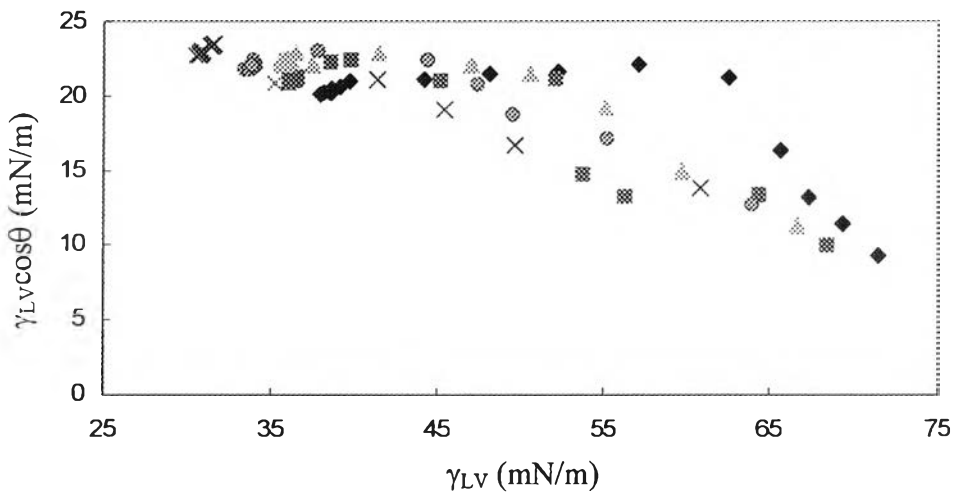

Figure 4.51 Adhesion tension plot for solutions of (♦) CPB, (×) $OP(EO)_{10}$, and their mixtures with α = (■) 0.25, (▲) 0.50, and (●) 0.75 on PC.

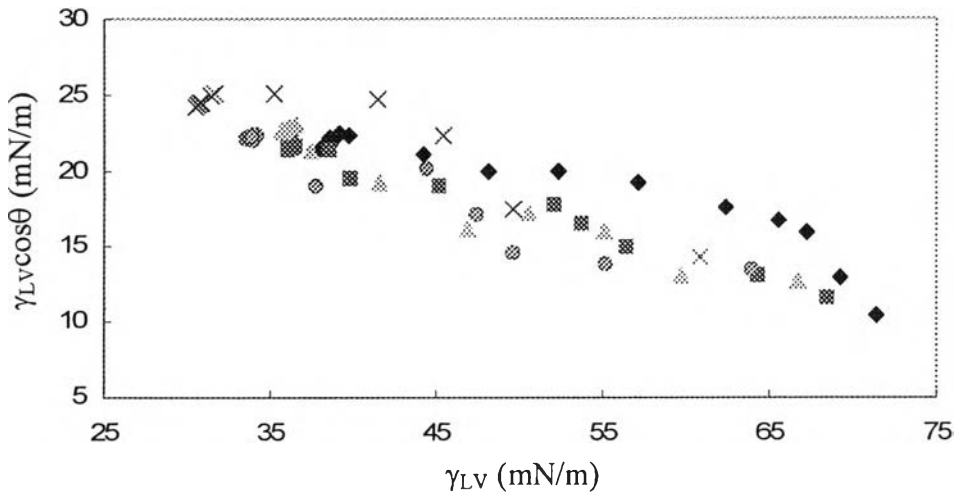

Figure 4.52 Adhesion tension plot for solutions of (♦) CPB, (×) $OP(EO)_{10}$, and their mixtures with α = (■) 0.25, (▲) 0.50, and (●) 0.75 on PVC.

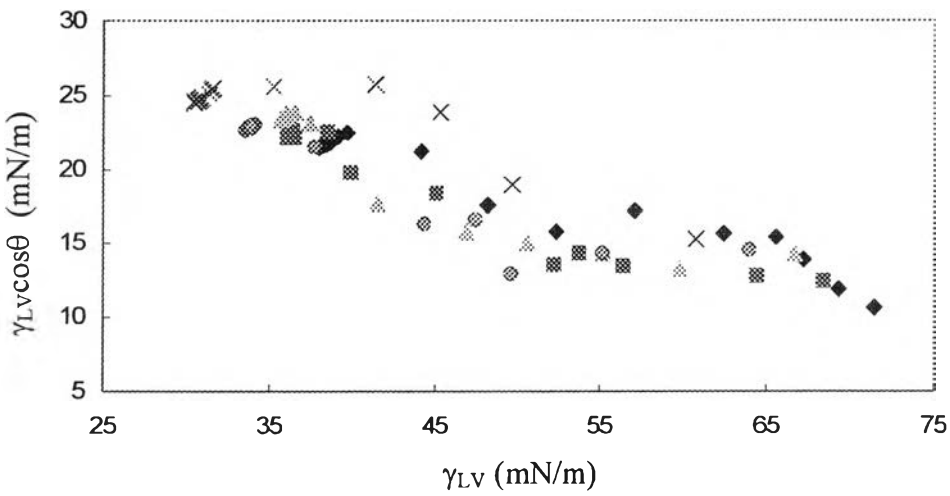

Figure 4.53 Adhesion tension plot for solutions of (♦) CPB, (×) $OP(EO)_{10}$, and their mixtures with α = (■) 0.25, (▲) 0.50, and (●) 0.75 on ABS.

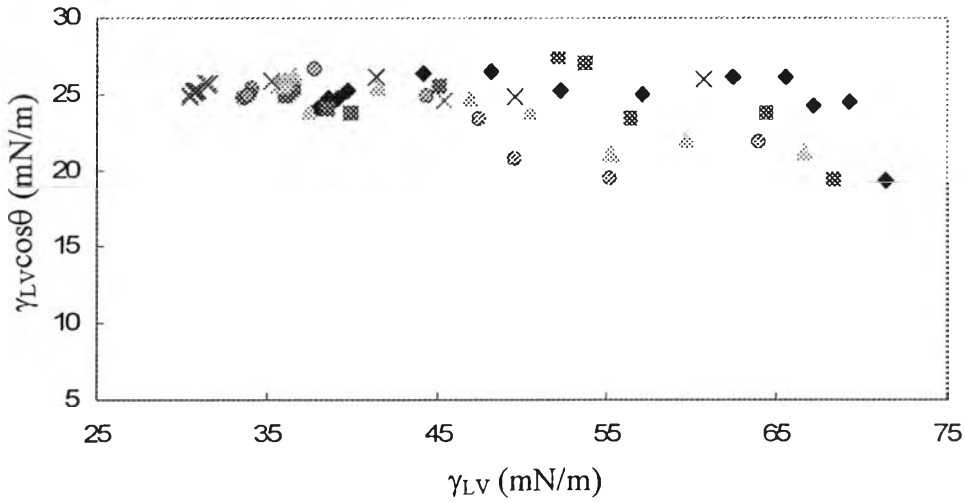

Figure 4.54 Adhesion tension plot for solutions of (♦) CPB, (×) $OP(EO)_{10}$, and their mixtures with α = (■) 0.25, (▲) 0.50, and (●) 0.75 on PMMA.

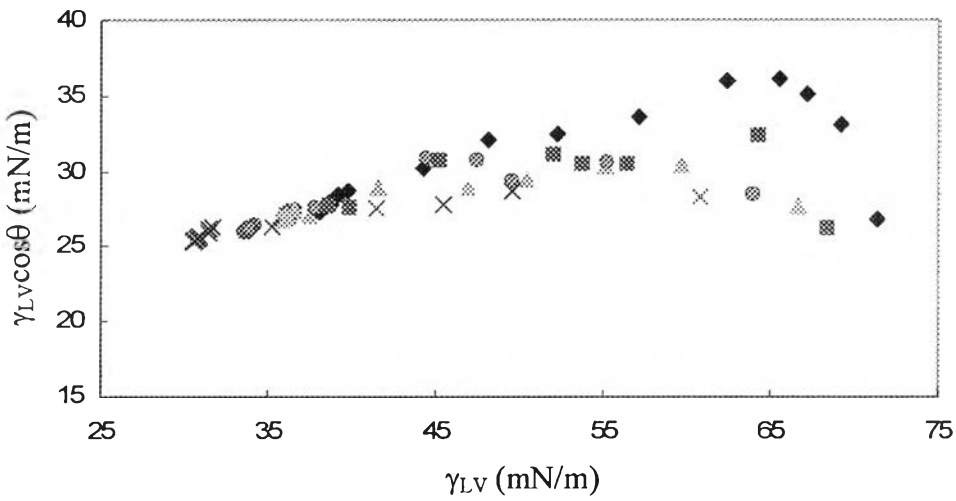

Figure 4.55 Adhesion tension plot for solutions of (♦) CPB, (×) $OP(EO)_{10}$, and their mixtures with α = (■) 0.25, (▲) 0.50, and (●) 0.75 on Nylon66.

The plots of cosθ versus γ_{LV}, are depicted in Figures 4.56 - 4.61, did not obviously deviate from the Zisman's plots. It could be explained that the nature of these plastic surfaces be considered as strong hydrophobic surfaces. As the results, the nature of the solid/liquid and the liquid/vapor interface was similar (Supalasate, 2004) and the addition of nonionic surfactant insignificantly affect to the wettability of surfactant solution that have the same γ_{LV}.

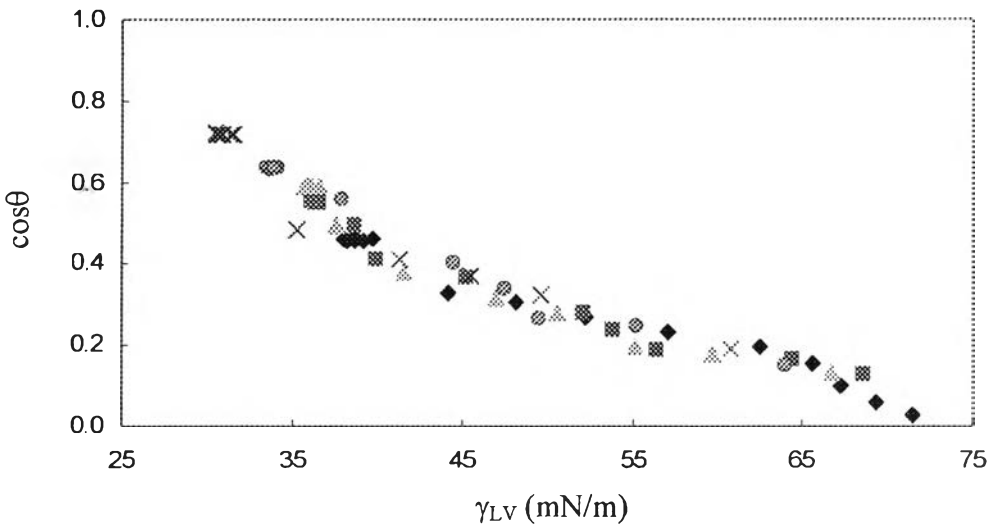

Figure 4.56 Contact angle for solutions of (♦) CPB, (×) $OP(EO)_{10}$, and their mixtures with α = (■) 0.25, (▲) 0.50, and (●) 0.75 on HDPE as a function of its γ_{LV}.

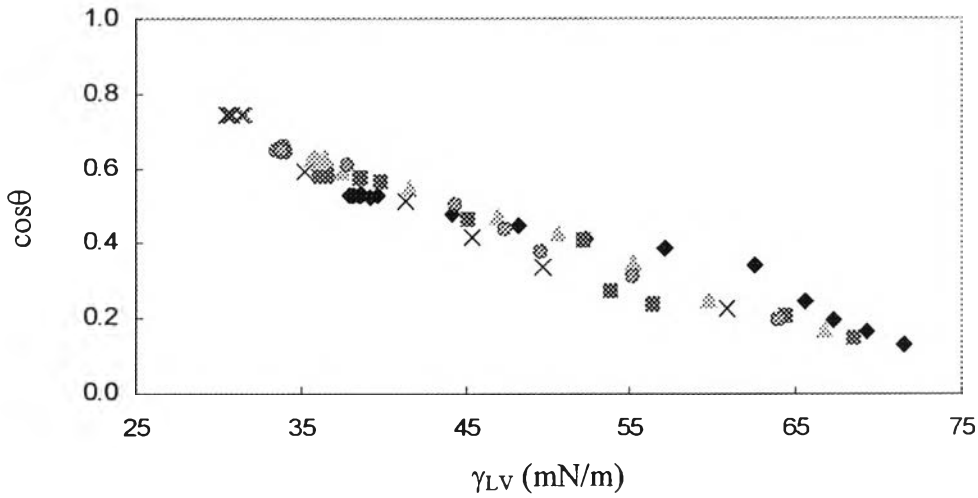

Figure 4.57 Contact angle for solutions of (♦) CPB, (×) $OP(EO)_{10}$, and their mixtures with α = (■) 0.25, (▲) 0.50, and (●) 0.75 on PC as a function of its γ_{LV}.

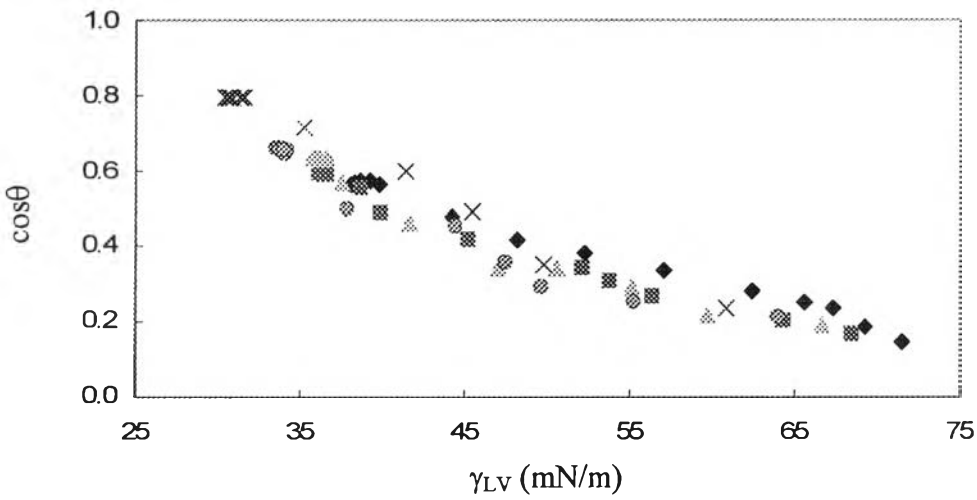

Figure 4.58 Contact angle for solutions of (♦) CPB, (×) $OP(EO)_{10}$, and their mixtures with α = (■) 0.25, (▲) 0.50, and (●) 0.75 on PVC as a function of its γ_{LV}.

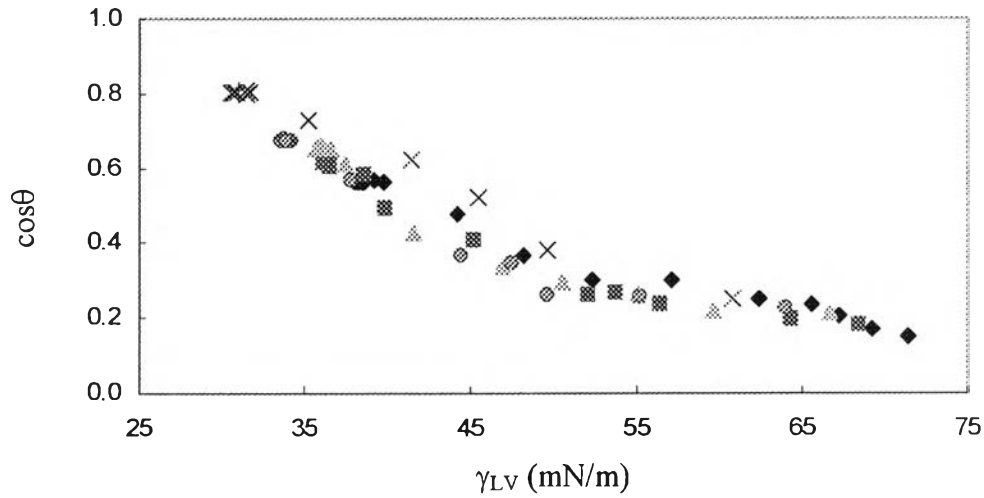

Figure 4.59 Contact angle for solutions of (♦) CPB, (×) $OP(EO)_{10}$, and their mixtures with α = (■) 0.25, (▲) 0.50, and (●) 0.75 on ABS as a function of its γ_{LV}.

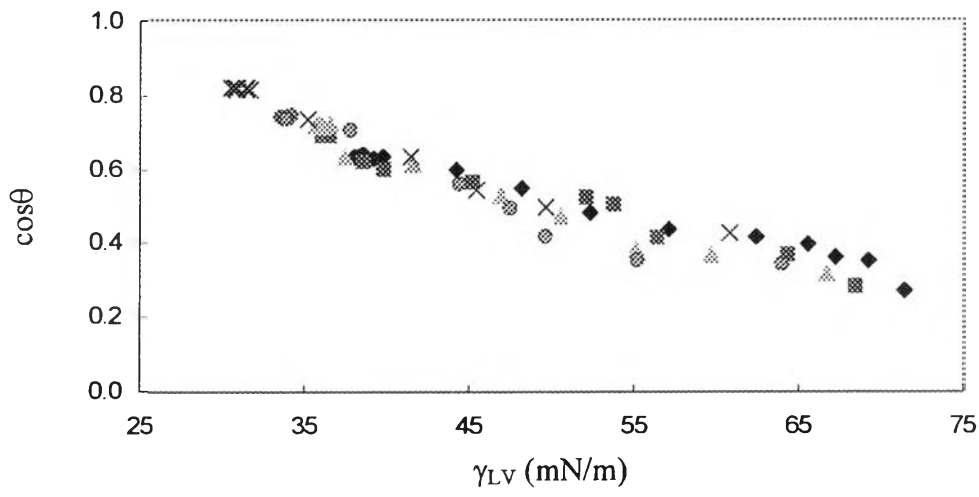

Figure 4.60 Contact angle for solutions of (♦) CPB, (×) $OP(EO)_{10}$, and their mixtures with α = (■) 0.25, (▲) 0.50, and (●) 0.75 on PMMA as a function of its γ_{LV}.

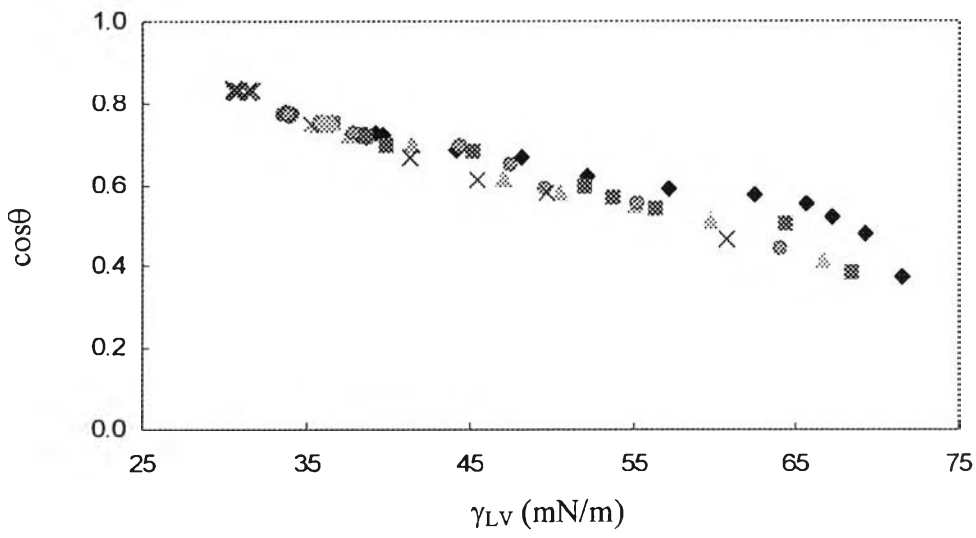

Figure 4.61 Contact angle for solutions of (♦) CPB, (×) $OP(EO)_{10}$, and their mixtures with α = (■) 0.25, (▲) 0.50, and (●) 0.75 on Nylon66 as a function of its γ_{LV}.